



Urolithin A induces cell cycle arrest and apoptosis by inhibiting Bcl-2, increasing p53-p21 proteins and reactive oxygen species production in colorectal cancer cells

Mohammad S. El-Wetidy^{1,2} · Rehan Ahmad³ · Islam Rady^{1,4} · Hamed Helal¹ · Mohamad I. Rady¹ · Mansoor-Ali Vaali-Mohammed³ · Khayal Al-Khayal³ · Thamer Bin Traiki³ · Maha-Hamadien Abdulla³

Received: 26 August 2020 / Revised: 15 December 2020 / Accepted: 21 December 2020 / Published online: 5 March 2021
© Cell Stress Society International 2021

Abstract

Colorectal cancer (CRC) is the second most common gastrointestinal cancer globally. Prevention of tumor cell proliferation and metastasis is vital for prolonging patient survival. Polyphenols provide a wide range of health benefits and prevention from cancer. In the gut, urolithins are the major metabolites of polyphenols. The objective of our study was to elucidate the molecular mechanism of the anticancer effect of urolithin A (UA) on colorectal cancer cells. UA was found to inhibit the cell proliferation of CRC cell lines in a dose-dependent and time-dependent manner in HT29, SW480, and SW620 cells. Exposure to UA resulted in cell cycle arrest in a dose-dependent manner along with alteration in the expression of cell cycle-related protein. Treatment of CRC cell lines with UA resulted in the induction of apoptosis. Treatment of HT29, SW480, and SW620 with UA resulted in increased expression of the pro-apoptotic proteins, p53 and p21. Similarly, UA treatment inhibited the anti-apoptotic protein expression of Bcl-2. Moreover, exposure of UA induced cytochrome c release and caspase activation. Furthermore, UA was found to generate reactive oxygen species (ROS) production in CRC cells. These findings indicate that UA possesses anticancer potential and may be used therapeutically for the treatment of CRC.

Keywords Colorectal cancer · Urolithin A · Cell cycle arrest · Apoptosis · Reactive oxygen species

Introduction

Colorectal cancer (CRC) is the predominant cancer of the digestive system and is, statistically, the third most commonly

diagnosed cancer globally, comprising 11% of all newly diagnosed cases, according to the GLOBOCAN 2018 database (Bray et al. 2018). Many factors contribute to the high incidence of CRC including obesity, sedentary lifestyle, and smoking which has increased the mortality rates of CRC. Cases in Eastern Europe, Latin America, and Asia have increased more than in other countries (Rawla et al. 2019).

Mohammad S. El-Wetidy and Rehan Ahmad contributed equally to this work.

✉ Rehan Ahmad
arehan@ksu.edu.sa

✉ Maha-Hamadien Abdulla
mabdulla@ksu.edu.sa

¹ Zoology Department, Faculty of Science, Al-Azhar University, Nasr City, Cairo 11823, Egypt

² College of Medicine Research Center, King Saud University, Riyadh 11461, Kingdom of Saudi Arabia

³ Colorectal Research Chair, Department of Surgery, College of Medicine, King Saud University, PO Box 7805 (37), Riyadh 11472, Kingdom of Saudi Arabia

⁴ Department of Dermatology, School of Medicine and Public Health, University of Wisconsin-Madison, Madison, WI 53706, USA

Multiple studies have reported the role of phytochemicals present in fresh fruits and vegetables in reducing the risk of CRC by inhibiting chemically induced colon carcinogenesis (Yin et al. 2016; Medic et al. 2019; Al-Ishaq et al. 2020). Fruits, nuts, grains, and vegetables contain polyphenols which have a cancer chemopreventive mechanism through a combination of their antiproliferative and pro-apoptotic properties (Moga et al. 2016). In the last two decades, polyphenols have been shown to have a wide spectrum of biological activities that modulate different signaling pathways including initiation, promotion, and progression of different types of cancers (Alam et al. 2018).

The ellagitannins are polyphenols which co-exist with the ellagic acid. They are produced by tannin hydrolysis in

pomegranates, strawberries, blueberries, and nuts and are characterized by their strong potential for development as chemopreventive agents against many types of human cancers (Ismail et al. 2016; Espín et al. 2013; Vicinanza et al. 2013; Ceci et al. 2018; Eskra et al. 2019). Urolithin A (UA) is the analog metabolite of the ellagic acid which is produced by the intestinal bacteria and considered the most active and effective metabolite possessing anti-inflammatory and antioxidant characteristics (Zhang et al. 2019). UA has been proven to potentiate the effect of 5-fluorouracil in colon cancer cells (González-Sarrías et al. 2015). Zhao and colleagues, in 2018, showed that UA induces autophagy and inhibits metastasis in a human colorectal cancer cell line SW620 (Zhao et al. 2018). Another study elucidated the antiproliferative capacity of UA by inhibiting glycolysis and modulating the p53-TIGAR axis in colorectal cancer cells (Norden and Heiss 2019).

UA may thus contribute to the treatment of various types of cancer and may represent an alternative or adjunct chemotherapeutic agent. The objective of this study was to evaluate and assess the chemopreventive activity of UA on colon cancer and to investigate its role as an antiproliferative and proapoptotic agent.

Materials and methods

Chemicals

The chemically synthesized compound UA was purchased from MedChemExpress LLC, NJ, USA, in a powder crystallized form, with more than 98% of purity. Dimethyl sulfoxide (DMSO), phosphate -buffered saline (PBS), glacial acetic acid, methanol, trypan blue, and propidium iodide (PI) were purchased from Sigma-Aldrich, St. Louis, MO, USA.

Preparation of UA

According to the manufacturer instructions, a 100-mM stock solution was prepared by dissolving in DMSO solvent, vortexed, centrifuged, aliquoted, and stored at -80°C , until use. Subsequently, the UA stock solution was re-diluted in DMSO to the required concentration, although the final concentration of DMSO in the culture medium did not exceed 1% as has been previously described (Zhao et al. 2018).

Cell culture

In the current study, HT29, SW480, and SW620 CRC cell lines (ATCC, Rockville, USA) were used. The effect of UA was tested in human fibroblast cells isolated from healthy tissues that had been used as a normal control in previous colon cancer studies (González-Sarrías et al. 2015, 2017a;

Aragonès et al. 2017). HT29 and SW480 cells were cultured and maintained in Dulbecco's Modified Eagle Medium (DMEM) (GIBCO, by Thermo Fisher Scientific, NY, USA) supplemented with 10% fetal bovine serum (FBS), 100 units/ml penicillin, and 100 μg streptomycin (González-Sarrías et al. 2016). SW620 and human fibroblast cells were cultured in Roswell Park Memorial Institute medium (RPMI-1640) (GIBCO, by Thermo Fisher Scientific, NY, USA) supplemented with 10% FBS and 1% penicillin and streptomycin (Napolitano et al. 2015). All cultures were incubated at 37°C in a humidified atmosphere of 5% CO_2 .

Measurement of cytotoxicity by MTT assay

The cytotoxicity effect of UA on the colon cancer cell lines HT29, SW480, and SW620 and on the normal human fibroblasts was measured by Cell Proliferation Kit I (MTT) (Sigma-Aldrich, St. Louis, MO, USA) according to the manufacturer's instructions. Briefly, cells were seeded in 96-well culture plates at 5000 cells/well for HT29 and 10,000 cells/well for the other types for 24 h. Cells were then incubated with various concentrations of UA (0, 3.125, 6.25, 12.5, 25, 50, 100, and 200 μM) for 24 h and 48 h at 37°C in a humidified 5% CO_2 incubator. At detection day, cells were incubated with MTT powder for 2 h after which violet crystals were formed at different color hues indicating cell metabolic activity. Colorimetric absorbance was measured at 620 nm (A620) and 570 nm (A570) by Synergy™ 2 Multi-Mode Microplate Reader (BioTek Inc., VT, USA). The cell viability was calculated as previously reported (Cho et al. 2015) using the following equation:

$$\text{Percentage of viability} = \frac{A570 - A620 \text{ of UA}}{A570 - A620 \text{ of the Control (0}\mu\text{M)}} \times 100$$

The half-maximal inhibitory concentration (IC_{50}) of UA, the concentration at which UA exerts half of its maximal inhibitory effect, was calculated by the IC_{50} calculator (AAT Bioquest, Inc., CA, USA) as previously described (Luparello et al. 2019). All experiments were performed in triplicate.

Cell cycle assay with propidium iodide

The effect of UA on the cell cycle was measured as described previously (Kim and Sederstrom 2015). Briefly, cells were seeded in 6-well plates (3×10^5 cells/well) and allowed to attach and grow for 24 h in the mean culture conditions. The cells were treated with UA (0, 25, 50, and 100 μM) for 24 h and 48 h. At the time of detection, cells were harvested and both the attached and floating cells were collected. The cells were fixed by slowly dropping 70% ice-cold ethanol and stored at 4°C for at least 30 min. Later, the cells were washed twice with ice-cold PBS, at 2000 rpm, then incubated in PBS with RNase A (10 mg/ml) (QIAGEN, Hilden, Germany) and

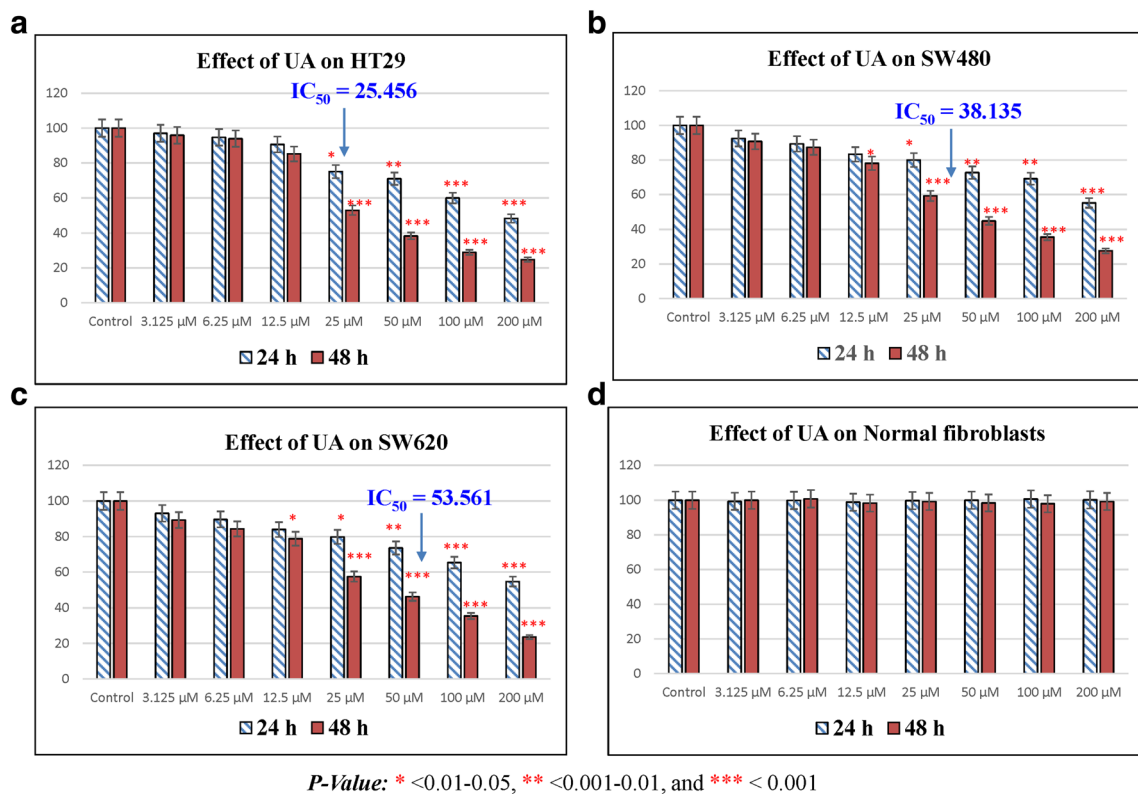


Fig. 1 Effect of UA on cell viability. Different concentrations of UA were used to study its effect on cell viability by MTT assay. Results of two time points at 24 h and 48 h were blotted and the IC_{50} were calculated for each

cell line. Data were considered significant if P values are < 0.05. **a** HT29. **b** SW480. **c** SW620. **d** Normal fibroblasts

PI (50 $\mu g/ml$) at room temperature for 10 min. Cell cycles were analyzed using a BD FACSCalibur™ Cell analyzer equipped with Cell Quest software at an emission > 575 nm (FL3). The area occupied by all the cell cycle phases (Sub G, G0/G1, S, and G2/M phases) was measured and graphed together as histograms.

Measurement of apoptosis by annexin V-FITC/PI assay

Induction of apoptosis was measured by Dead Cell Apoptosis Kit with annexin V-FITC and PI, for flow cytometry (Invitrogen, by Thermo Fisher Scientific, OR, USA) according to the manufacturer's instructions. Cells were seeded in a 6-well plate (3×10^5 cells/well) and treated with the UA (0, 25, 50, and 100 μM) for 24 h and 48 h. Both floating and adherent cells were harvested, pooled together, and incubated with annexin V-FITC and PI for 15 min on ice in the dark. The cells were analyzed by BD FACSCalibur™ cell analyzer (BD Biosciences, CA, USA) at an emission of 530 nm (FL1 channel) and > 575 nm (FL3). The percentage of live cells (negative in both annexin V-FITC and PI), early apoptotic (positive in annexin V-FITC), late apoptotic and completely dead (positive in both annexin V-FITC and PI), and necrotic cells (only positive for PI) were all calculated and graphed together as reported previously (Crowley et al. 2016).

Reactive oxygen species assay

The oxidative stress effect induced by UA through the reactive oxygen species (ROS) production was tested by the DCFDA/H2DCFDA-Cellular ROS Assay Kit (ABCAM, Cambridge, UK) and flow cytometer according to the manufacturer's instructions, as described previously (Degl'Innocenti et al. 2019). In the current study, all cell types were seeded in 6-well plates (3×10^5 cells/well) and were allowed to attach for 24 h as described above. The cells were treated with UA (0, 50, and 100 μM) for 24 h. At the detection time, cells were trypsinized and all of the attached and floating cells were collected. The cells were then treated by 2',7'-dichlorofluorescein diacetate (DCFDA) and stored at 37 °C for 30 min. Before the analysis, the cells were twice washed with ice-cold PBS and analyzed using a flow cytometer at an emission of 530 nm (FL1 channel) and 150 mV.

Western blot analysis

All cells were seeded in a 100-mm dish (1×10^6 cells/dish) up to 50% confluency in 5% CO_2 at 37 °C in the appropriate culture medium. The cells were treated with UA (0, 25, 50, and 100 μM) for 48 h. On the experiment day, cells were washed with $1 \times$ PBS, harvested, and lysed in RIPA lysis buffer,

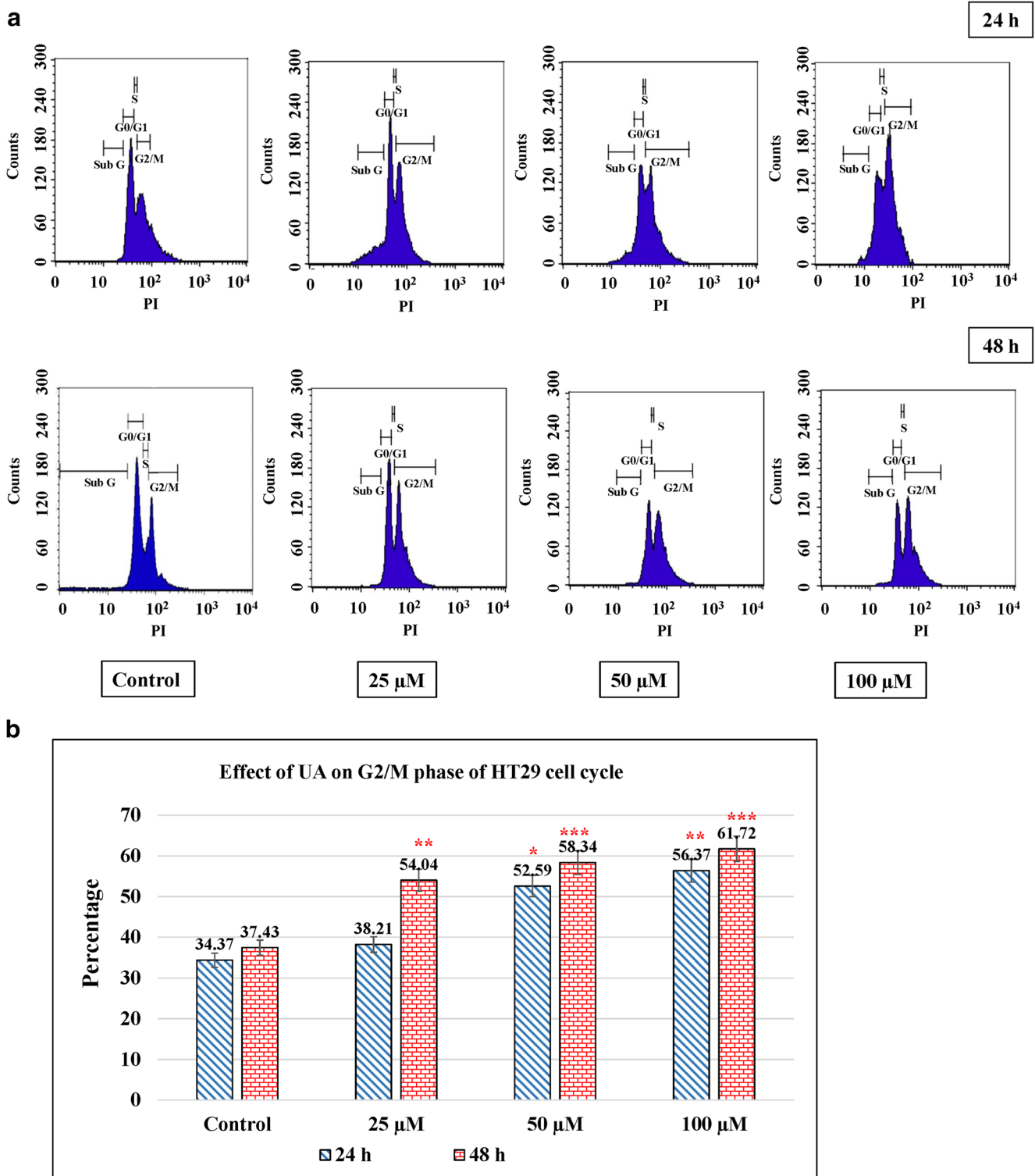


Fig. 2 Effect of UA on the cell cycle. Three concentrations of UA (25 μ M, 50 μ M, and 100 μ M) in addition to one untreated plate as a control were used to test its effect on the cell cycle by PI in the three cancer cell lines in addition to the normal fibroblasts. Cells were treated with the mean concentration for 24 h and 48 h. Sub G1, G0/G1, S, and

G2/M phases were detected for each cell type, and the statistical analysis was performed where the significance of data was assessed at P value < 0.05. Bar charts were created to compare the effect of UA on the G2/M phase into the two different time intervals and the percentage cells were indicated. **a, b** HT29. **c, d** SW480. **e, f** SW620. **g** Normal fibroblasts

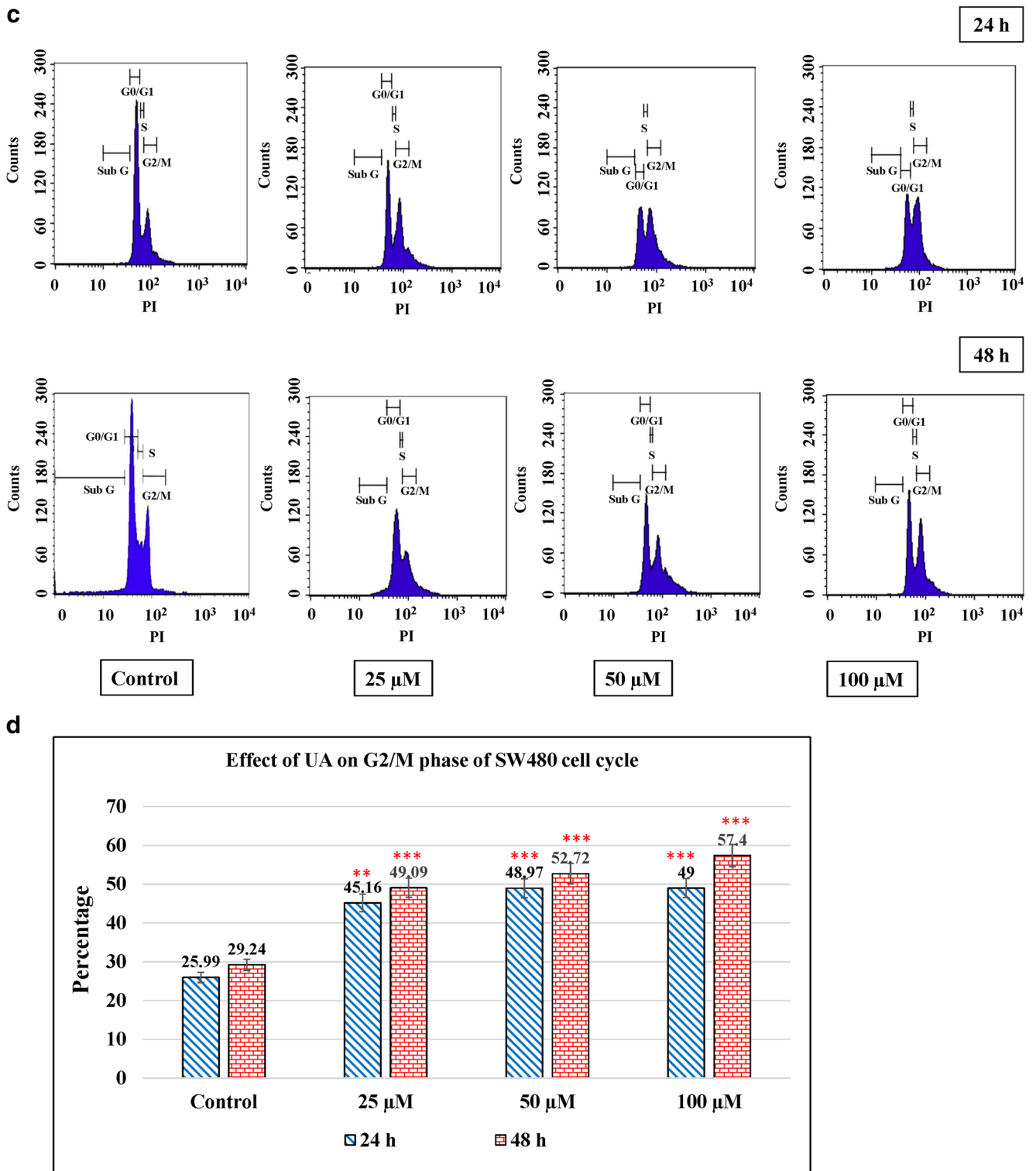
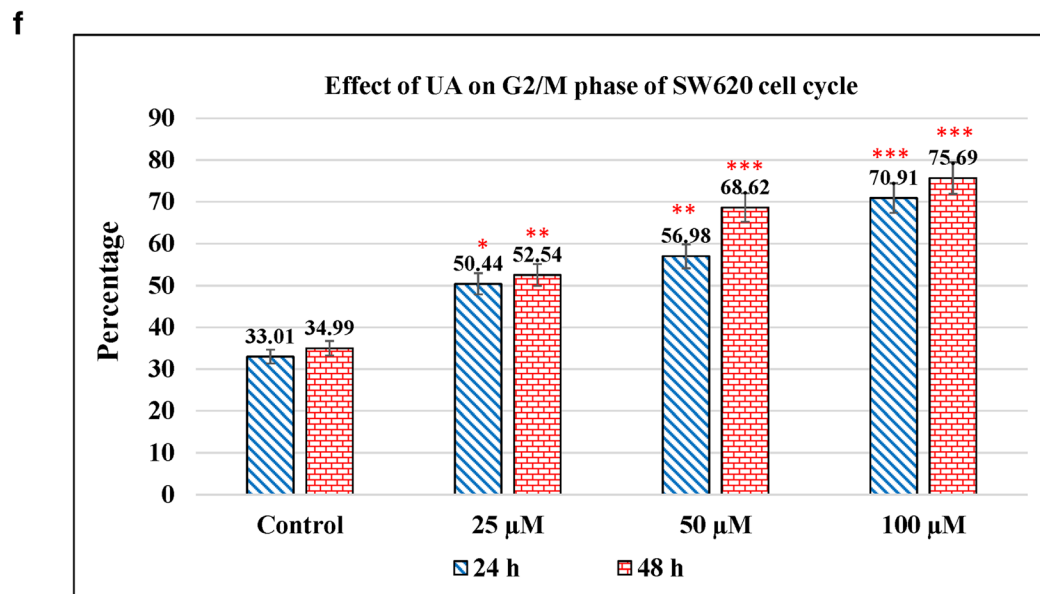
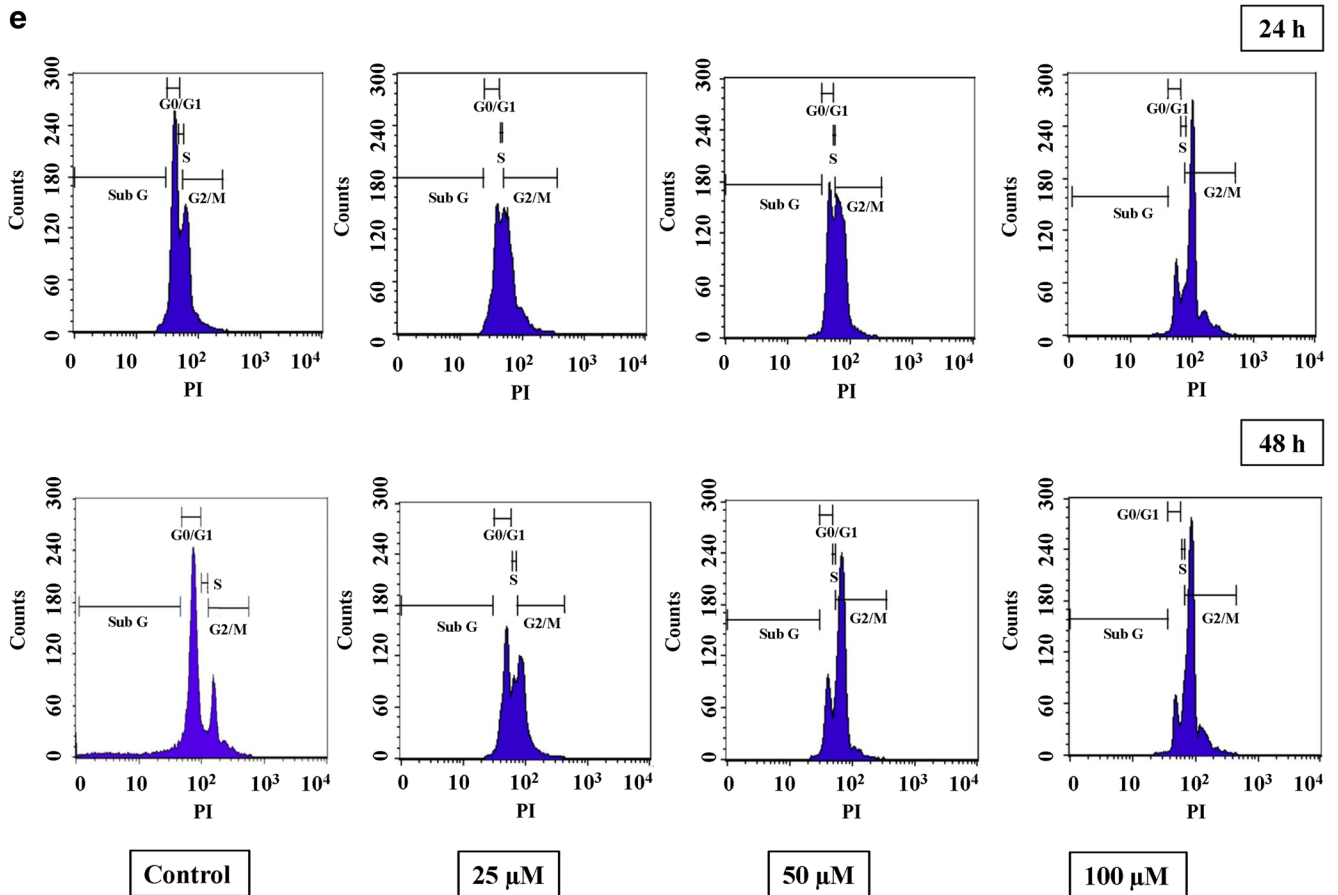


Fig. 2 continued

combined with protease inhibitors (Sigma-Aldrich, St. Louis, MO, USA) according to the manufacturer’s instructions. The total protein concentration was evaluated by the colorimetric

Bradford protein assay (BIO-RAD Inc., CA, USA) at 595-nm absorbance. Lysates were loaded in equal concentrations and separated by sodium dodecyl sulfate-polyacrylamide gel



P-Value: * <0.01-0.05, ** <0.001-0.01, and *** <0.001

Fig. 2 continued

electrophoresis (SDS-PAGE) and then transferred to a nitrocellulose membrane by a semi-dry technique as described

elsewhere (Cai et al. 2018). Blocking of the membrane was done by 5% non-fat dried milk for 1 h and incubated with the

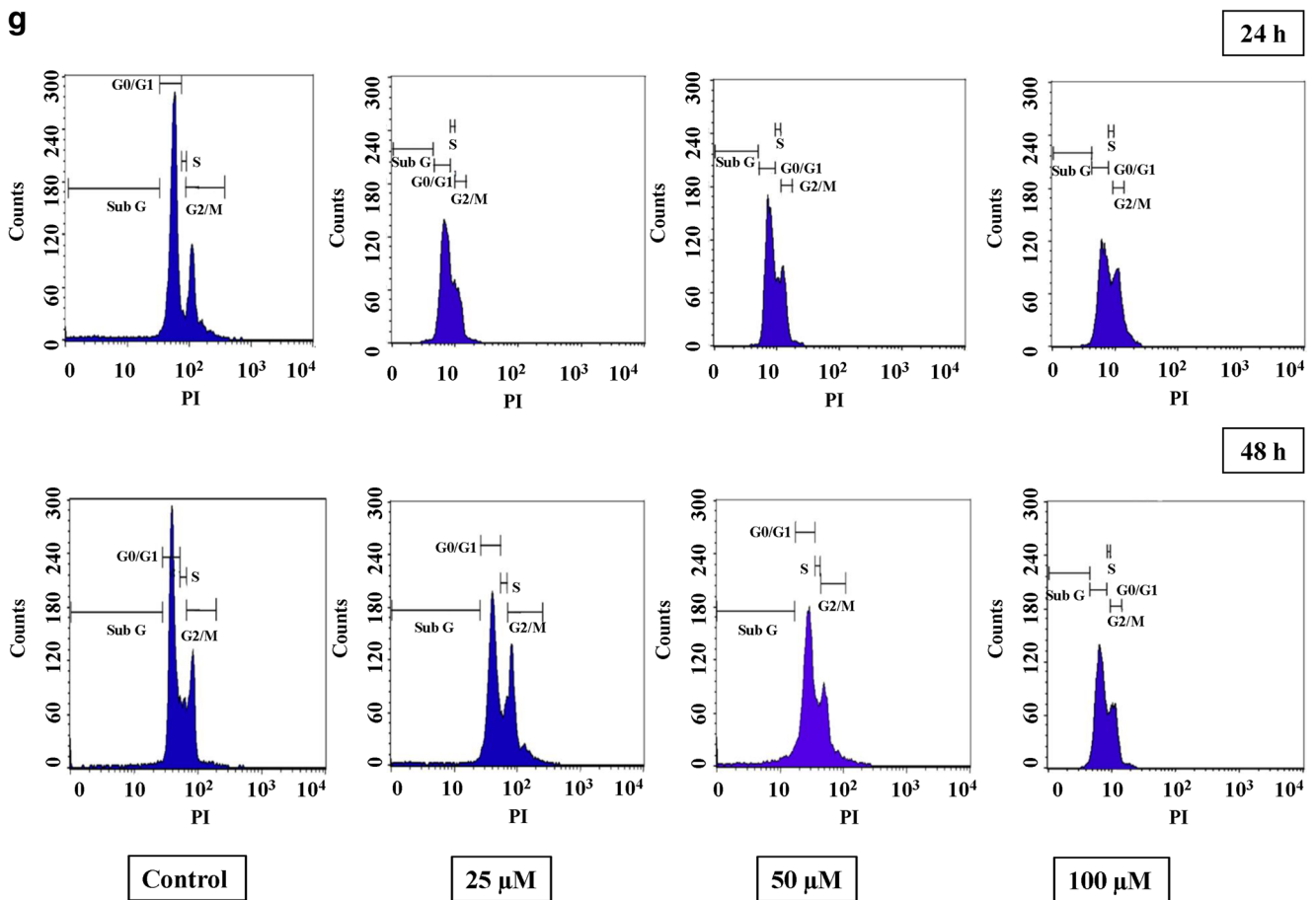


Fig. 2 continued

primary antibodies to CDK6 (cat. no. PA5-27978) from (Invitrogen, by Thermo Fisher Scientific, OR, USA), cytochrome C (cat. no. sc-13156), caspase-3 (cat. no. sc-271028), caspase-9 (cat. no. sc-17784), XIAP (cat. no. sc-28537), p53 (cat. no. sc-6243), p21 (cat. no. sc-6246), Bcl-2 (cat. no. sc-7382), cyclin B1 (cat. no. sc-70898), and β Actin (cat. no. sc-69879) from (Santa Cruz Biotechnology, Inc., Dallas, TX, USA). The secondary antibodies used were goat anti-mouse IgG-HRP (cat. no. sc-2005) and mouse anti-rabbit IgG-HRP (cat. no. sc-2357) from (Santa Cruz Biotechnology, Inc., Dallas, TX, USA). Chemiluminescence was detected using Luminol HRP chemiluminescence substrate (cat. no. sc-2048) from Santa Cruz Biotechnology, Inc., Dallas, TX, USA, and then visualized by c-digit blot-scanner (LI-COR, NE, USA). Band's intensity was mathematically measured by ImageJ software version 1.51.8 (National Institutes of Health, USA).

Statistical analysis

The statistical analysis by the one-way ANOVA test was performed by SPSS software, version 21 (SPSS Inc., Chicago,

IL, USA). Results were considered significant if the *P* values were < 0.05.

Results

UA inhibits the proliferation of human CRC cell lines

In the current study, the effects of UA on colon cancer cell viability were assessed by MTT. HT29 cells were treated with different concentrations of UA starting from 3.125 μM and up to 200 μM for 24 h and 48 h. The results were compared with those of the untreated control cells to estimate their antiproliferative efficacy. UA was found to inhibit proliferation at 25 μM increasing up to 200 μM . UA significantly inhibited the proliferation of HT29 in a dose-dependent manner, although lower concentrations of UA were found to have no significant effect. The calculated IC_{50} of UA for its effect on HT29 was 25.45 μM (Fig. 1a). Another adenocarcinoma cell line SW480 cell proliferation was inhibited by UA in a dose-dependent manner (Fig. 1b), and the calculated IC_{50} was

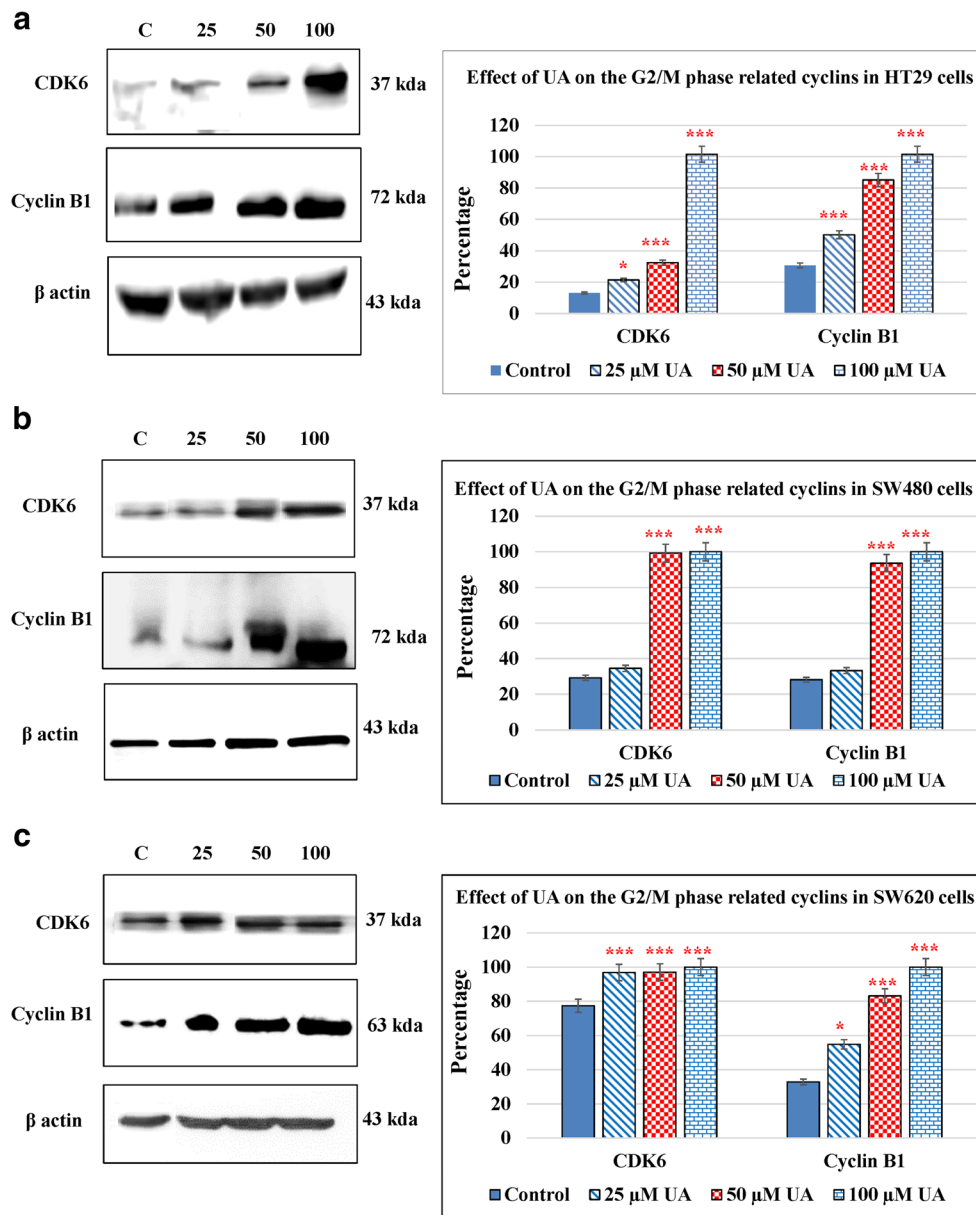


Fig. 3 UA modulates cell cycle-related proteins. The effect of UA on the G2/M phase-related cyclins was shown. The cells were treated for 48 h with UA in a dose-dependent manner. The band intensities were calculated by NIH Image J software and the bar charts were created to compare

the effect of UA on G2/M phase-related proteins. The statistical analysis was performed where the significance of data was assessed at a *P* value < 0.05. **a** HT29. **b** SW480. **c** SW620

38.135 μM. SW620 is a metastatic colorectal cancer cell line derived from the same patients as that of SW480. The effect of UA was studied on SW620. As expected UA was found to inhibit cell proliferation in a dose-dependent manner. Metastatic cancer cells seemed to resist the UA as compared to adenocarcinoma cell lines. The IC_{50} was calculated to be 53.561 μM in SW620 cells (Fig. 1c). The dose-dependent treatment by UA did not affect the proliferation of normal fibroblasts at both time intervals (Fig. 1d). These findings indicated that UA was found to inhibit the proliferation of

CRC cell lines without affecting normal fibroblasts (Supplementary Table 1).

UA induces cell cycle arrest at G2/M phase

To understand the effect of UA on cell cycle distribution, HT29 cells were treated with different concentrations of UA. Cell cycle distribution was measured using propidium iodide. The results showed that UA altered the cell cycle in HT29 by reducing the G0/G1 population and accumulation of cells at the G2/M phase

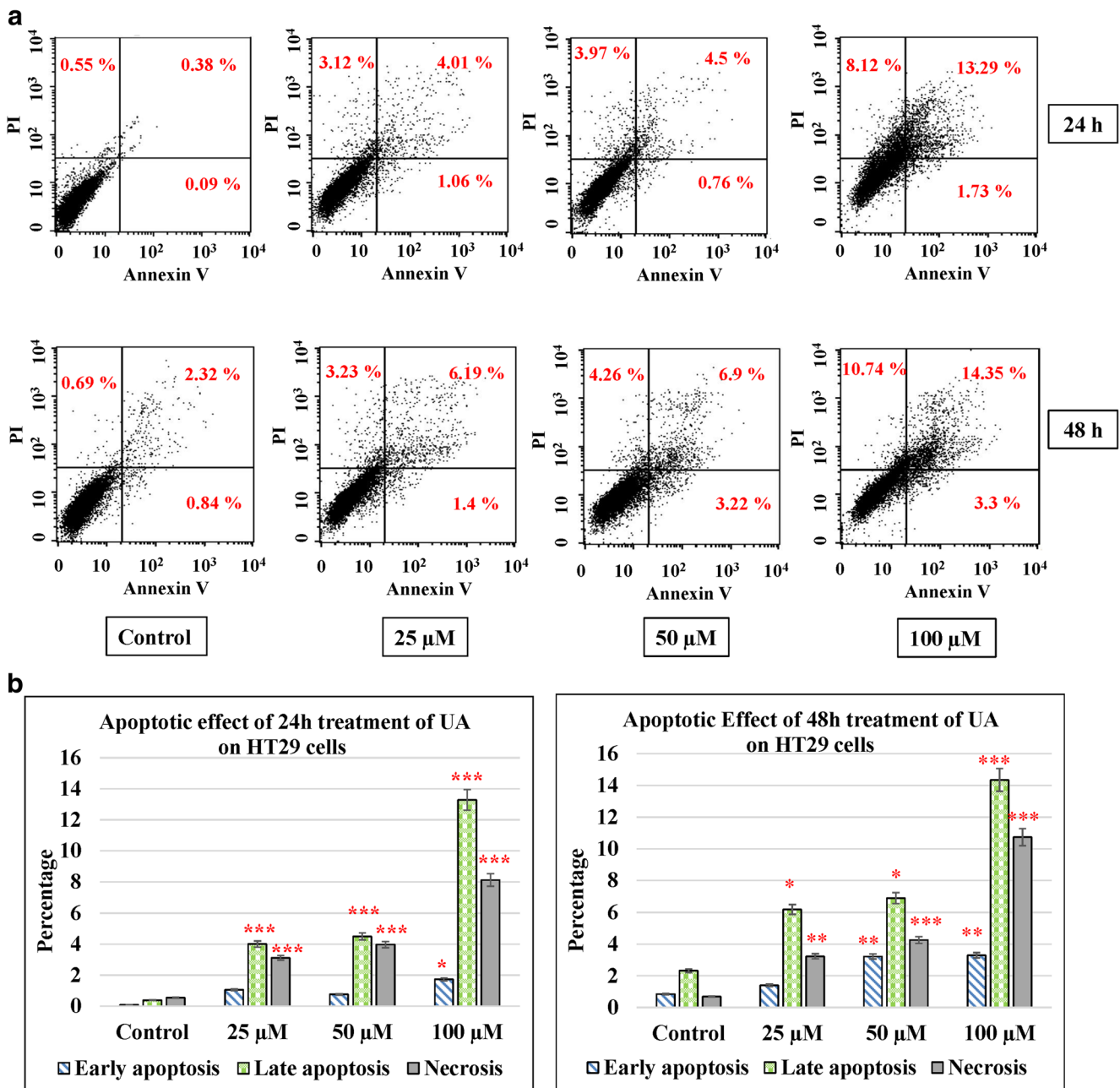


Fig. 4 UA induces apoptosis. Three concentrations of UA (25 μM, 50 μM, and 100 μM) in addition to one untreated plate as a control were used to test the apoptotic effect by using annexin V and propidium iodide (PI) in the three cancer cell lines in addition to the normal fibroblasts. Cells were treated with the mean concentration for

24 h and 48 h. Quadrant was set for the resulted dots population depending on the results of the negative auto-fluorescence, and the statistical analysis was performed where the significance of data was assessed at *P* value < 0.05. **a** and **b** HT29. **c** and **d** SW480. **e** and **f** SW620. **g** and **h** Normal fibroblasts

at 24 h and 48 h (Fig. 2a, b). In UA-exposed HT29 cells, the peak of the G2/M phase increased, gradually and significantly, in a dose-dependent manner, up to 50% at 24 h (*P* < 0.01) and 64% at 48 h (*P* < 0.001) in the 100 μM as shown (Fig. 2a). Similarly, in SW480 cells treated with UA, the peak of the G2/M phase increased significantly, in a dose-dependent manner, up to 67.5% at 24 h (*P* < 0.001) and 96% at 48 h (*P* < 0.001) in the 100-μM setting as shown in (Fig. 2c, d). A similar result was obtained in

SW620 cells. Treatment of SW620 cells with UA resulted in the depletion of the G0/G1 phase with significant accumulation of G2/M at 24 h and 48 h (Fig. 2e, f). However, there was no significant alteration of the cell cycle in UA-treated normal fibroblasts (Fig. 2g). These findings demonstrate that UA-induced inhibition of cell proliferation was mediated by cell cycle arrest, Supplementary Table 1.

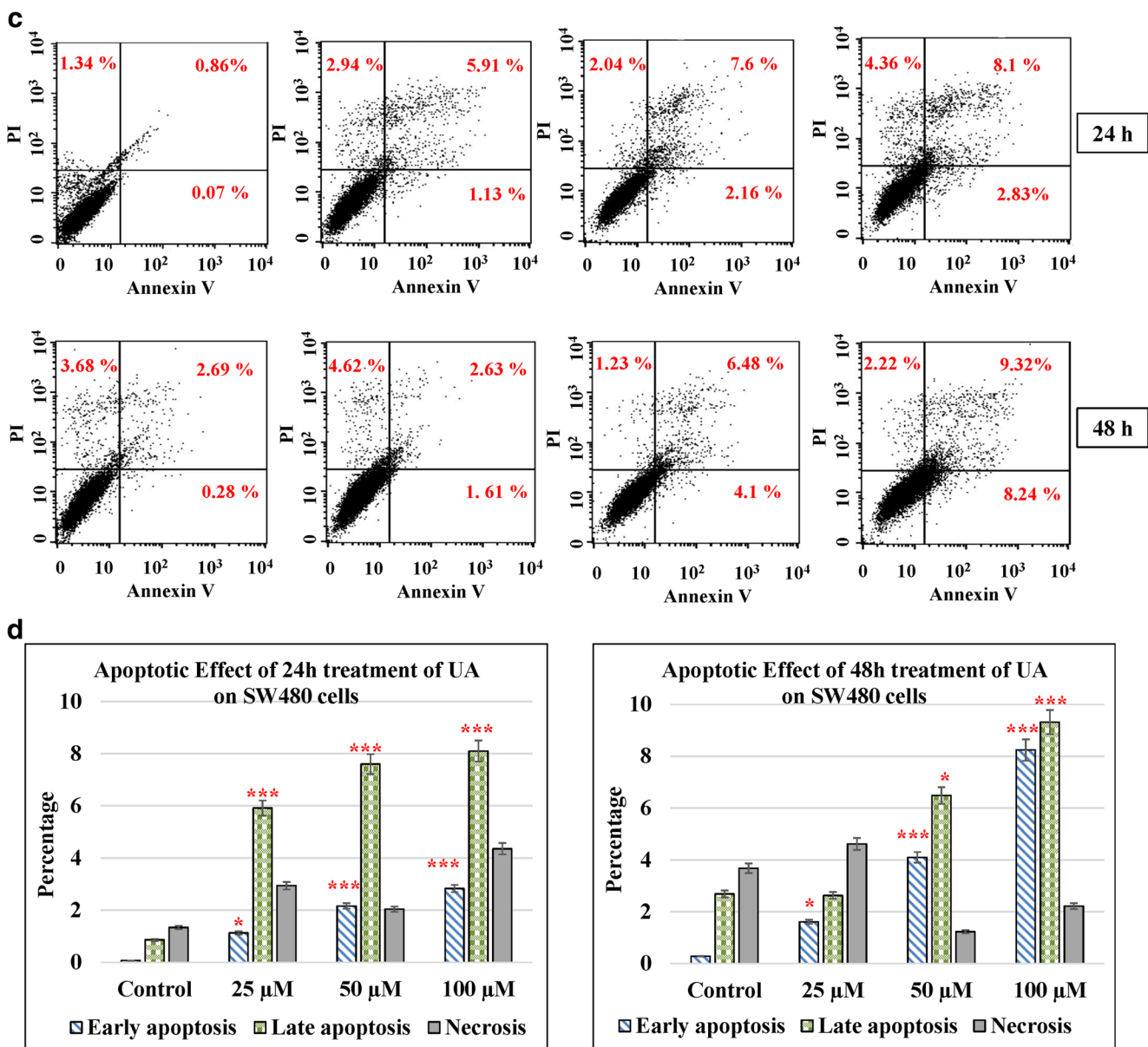


Fig. 4 continued

UA modulates cell cycle-related protein

To investigate the effect of UA on cell cycle arrest, we further analyzed the impact of UA on cell cycle regulators. The cell cycle progresses by activation of a complex of cyclin and cyclin-dependent kinases (CDKs). The effect of UA was studied on cyclin B1 and CDK6 as they play a vital role in the regulation of the G2/M phase (Bai et al. 2017). Treatment of HT29 cells with different concentrations of UA resulted in a marked increase in cyclin B1 as compared to control cells. HT29 treated with UA resulted in a significant increase in the levels of CDK6 which indicated a robust cell cycle accumulation at the G2/M phase (Fig. 3a). Similarly, SW480 cells treated with different

concentrations of UA resulted in a significant increase in cyclin B1 and CDK6 (Fig. 3b). A similar result was obtained in a metastatic CRC cell line SW620 (Fig. 3c).

UA induces cancer cell apoptosis

Apoptosis in cells occurs during normal development and turnover, as well as in a variety of pathological conditions. Dysregulation of apoptosis contributes to disorders such as cancer, viral infection, autoimmune diseases, neurodegenerative disorders, and stroke. Cancer cells inhibit apoptosis for their survival. Most of the anticancer drugs kill cancer cells by inducing apoptosis. Many cancer cells also developed

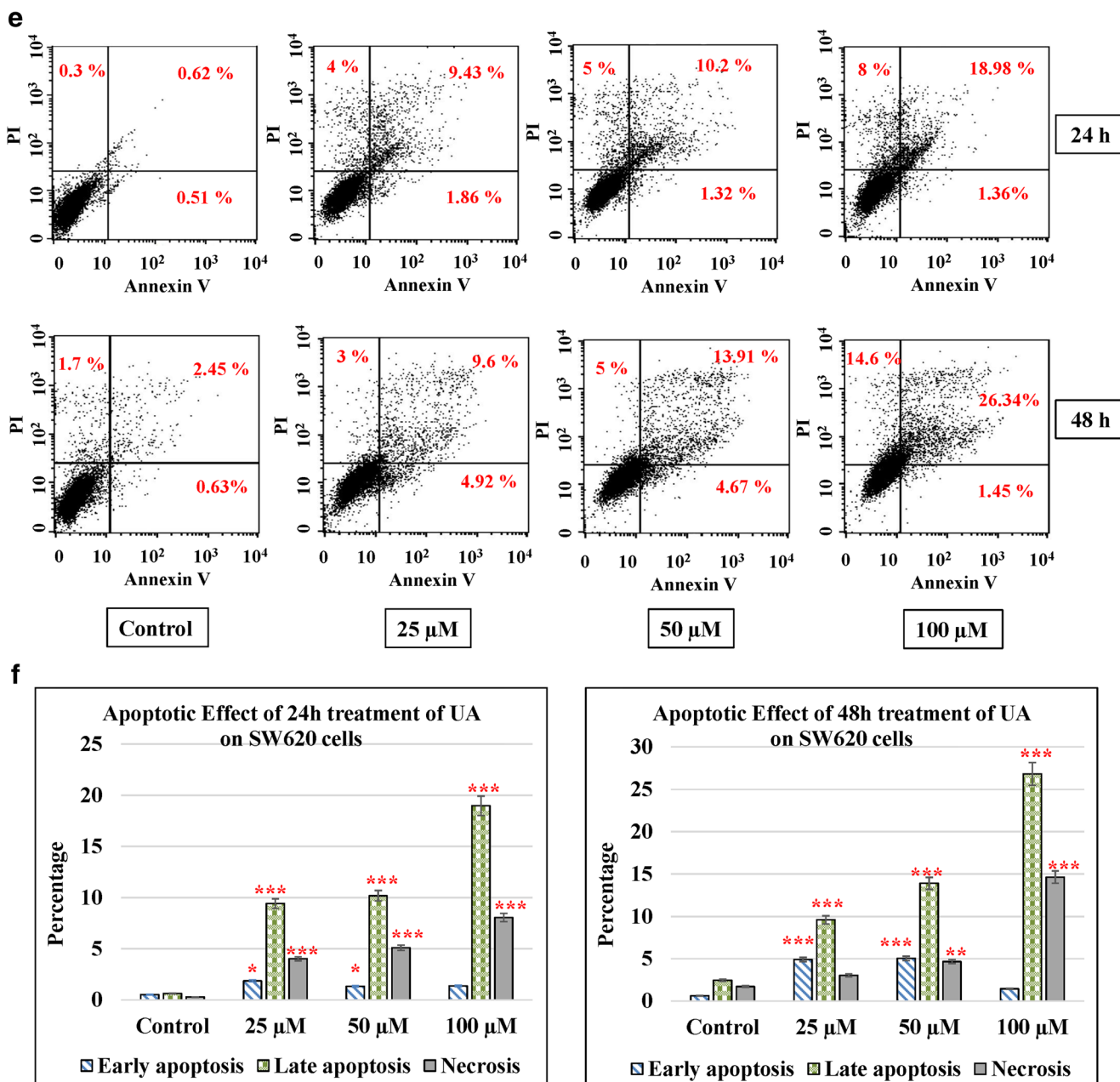


Fig. 4 continued

resistance to certain drugs by blocking apoptosis. In the current study, we evaluated the effect of UA on apoptosis by annexin V/PI assay in colon cancer cells. We used different concentrations of UA (25, 50, and 100 μM) at 24 h and 48 h. HT29 treated with UA induced significant late apoptosis ($P < 0.001$) at 24 h (13.3%) and 48 h (14.35%) compared to the control (2.32%). The early apoptosis increased fourfold at 100 μM of UA after 48 h (3.32%) compared to the control (0.83%) (Fig. 4a, b). The effect of UA on SW480 was similar where 100 μM of UA induced a threefold increase after 24 h (8.1%) and fourfold after 48 h (9.32%) compared to the control (2.69%). At the same time, the early apoptosis was

significantly ($P < 0.001$) much stronger by 10-fold increases after 24 h (2.39%) and 40-fold increases after 48 h (8.24%) post-treatment, compared to the control (0.28%) (Fig. 4c, d). The maximum effect of UA was observed in SW620 cells, where 100 μM of UA significantly increased the percentage of late apoptosis to 19.89% at 24 h and to 26.34% at 48 h ($P < 0.001$) compared with 2.45% of the control. Additionally, the PI percentages increased up to 14.36% in cells treated with 100 μM of UA compared to 1.71% of the control (Fig. 4e, f). Moreover, UA showed no significant effect on the normal fibroblasts (Fig. 4g, h).

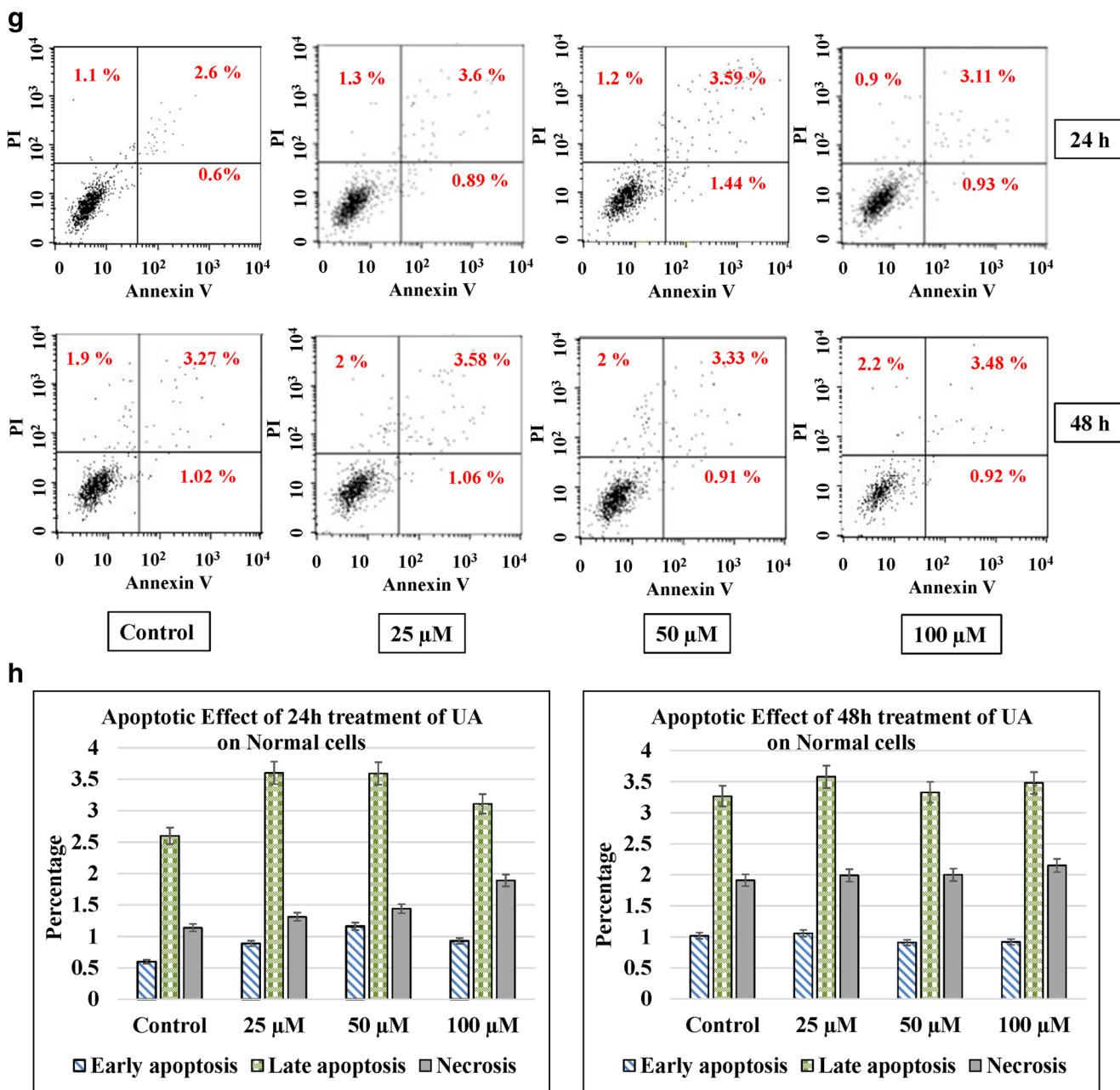


Fig. 4 continued

UA increases pro-apoptotic protein and inhibits anti-apoptotic protein expression

The balance between pro-apoptotic and anti-apoptotic determines cell fate under stress. To confirm the apoptotic effect induced by UA, the expression of some regulatory proteins which are involved in either the extrinsic or intrinsic apoptotic pathways were evaluated. Cytochrome c, which is associated with the inner membrane of the mitochondria with a key role in ATP production (Kühlbrandt 2015), the tumor suppressor

p53 (Liu et al. 2019), the cell cycle inhibitor p21 (El-Deiry 2016), the x-linked inhibitor of apoptosis XIAP (Tchoghandjian et al. 2016), the anti-apoptotic protein Bcl-2 (Campbell and Tait 2018), the apoptosis executioner caspase-3 (Crowley and Waterhouse 2016), and the apoptosis initiator Caspase-9 (Li et al. 2017) were studied. Treatment of HT29 cells with different concentrations of UA resulted in the inhibition of anti-apoptotic protein Bcl-2 and XIAP (Fig. 5a, b). p53 is a tumor suppressor critical for apoptosis. UA treatment resulted in the upregulation of p53 and its target gene p21

(Fig. 5a, b). Cytochrome c release from mitochondria into cytosol results in the activation of the caspase cascade. UA-treated HP29 cells enhanced the cytochrome c expression as compared to control (Fig. 5a, b). Exposure of HT29 to different concentrations of UA exhibited an increase in cleaved caspase-3 and caspase-9 (Fig. 5a, b). Exposure of SW480 cells to UA treatment resulted in the depletion of Bcl-2 and XIAP and upregulation of p53 and p21. UA treatment increased the levels of cytochrome c, cleaved caspase-3, and cleaved caspase-9 significantly in a dose-dependent manner (Fig. 5c, d). UA-exposed SW620 cells exhibited elevated levels of cytochrome c, cleaved caspase-3, cleaved caspase-9, p53, and p21 significantly in a dose-dependent manner (Fig. 5e, f). These findings thus indicate that UA-induced apoptosis is mediated by inhibiting anti-apoptotic proteins and increasing the pro-apoptotic protein expression. UA treatment of normal fibroblasts resulted in no alteration in XIAP and p21 (Fig. 5g, h) indicating the effectiveness and specificity of UA towards cancer cells.

UA increases ROS production and induces oxidative cellular stress

Cellular proliferation and survival need a certain level of ROS. Under physiological conditions, a certain amount of ROS is required to maintain the balance of proliferation and apoptosis of cells. An excessive amount of ROS results in ROS-mediated signaling cascades increasing the chances of cell death and inhibiting cell growth. UA treatment of HT29 resulted in a significantly increased generation of ROS in a dose-dependent manner at *t* 24 h (Fig. 6a). Exposure of SW480 to UA increased the production of ROS in a dose-dependent manner at 24 h (Fig. 6b). A similar result was obtained in SW620 treated with UA (Fig. 6c). Moreover, UA treatment exhibited no production of ROS in fibroblast cells; instead, it decreased its accumulation compared to the untreated cells (Fig. 6d). As ROS generation is mostly an early event, analysis of ROS at early time points indicated that ROS production was found at 2–4 h in UA-treated HT-29 cells. Generation of ROS was noticed at 24 h post-UA-treatment in SW480 cells. However, in metastatic cell line SW620, production of ROS was observed at a later time point (48 h) (Supplementary Fig. 1). These findings indicate that UA-mediated ROS production is an early event leading to apoptosis in adenocarcinoma cells. However, metastatic cells were found to resist but eventually elicited ROS at a later time after apoptosis induction.

Discussion

Over the last four decades, the management of CRC, and probably other cancers, has depended mainly on the usage of different types of chemotherapies such as oxaliplatin, fluorouracil,

and leucovorin (André et al. 2015; Conteduca et al. 2018; Degirmencioglu et al. 2019). Despite substantial progress in the treatment of a variety of tumors by these chemotherapies, some clinical studies have reported adverse side effects while others have demonstrated the persistence of cellular resistances as well (Hammond et al. 2016; Zhang et al. 2016; Van der Jeught et al. 2018; Conteduca et al. 2018). Recent studies have reported the use of some types of phytochemicals, naturally occurring compounds such as dietary polyphenols, which have been used successfully in the prevention and treatment of some types of cancer including CRC (Afrin et al. 2020; Ahmed et al. 2019). In the current study, we used urolithin A (UA), a product of ellagitannin metabolism by the gut bacteria, as a possible treatment for colorectal cancer.

In this study, UA decreased the viability and proliferation in the three CRC cell lines while it had a non-significant effect on the normal fibroblast cells. These results proved its robust antiproliferative effect on tumorigenic cells at different IC₅₀ doses. Previous studies have reported a similar effect of UA on SW620 (Zhao et al. 2018), HT29 (Cho et al. 2015; González-Sarriás et al. 2016; Kasimsetty et al. 2010), Caco-2 (González-Sarriás et al. 2017b), and SW480 (González-Sarriás et al. 2016); UA induced a limited effect on the normal colon fibroblast cell line CCD18-Co alone or in combination with other compounds such as ellagic acid, and urolithin B (González-Sarriás et al. 2010) or at higher concentrations and longer incubation periods (González-Sarriás et al. 2017b). These results assess the safety of UA in normal cells. In contrast to cancer cell lines, it did not affect the normal fibroblasts which are in agreement with previous findings. In vivo studies suggested that UA is not genotoxic (Heilman et al. 2017) and that it might have a protective role against ulcerative colitis which is a risk factor for developing CRC (Larrosa et al. 2010; Yuzugulen et al. 2019).

Moreover, UA induced significant cellular apoptosis in all CRC cells, in a dose-dependent manner and at two-time intervals. Apoptosis or programmed cell death is implicated in different disease states, such as neurodegeneration disease and cancer (Zhang et al. 2018). In the present study, we used the annexin V/PI assay to investigate the apoptotic role of UA on colon cancer cells. Annexin V has a high affinity for phosphatidylserine (PS) which is reported to occur on the external cell surface in the early phases of apoptotic cell death (Menyhárt et al. 2016).

The results showed that UA induced a highly significant late and early apoptosis in all cancer cells in a dose-dependent manner. In CRC, several studies show UA induced early and late apoptosis in Caco-2 and SW480 cells (González-Sarriás et al. 2017a, b), HT29 cells (Cho et al. 2015), SW620 cells (Zhao et al. 2018), and HCT116 cells (Norden and Heiss 2019) which are in agreement with our findings. Other studies reported the induction of apoptosis upon treatment with different doses of UA in different types of cancers, such as in

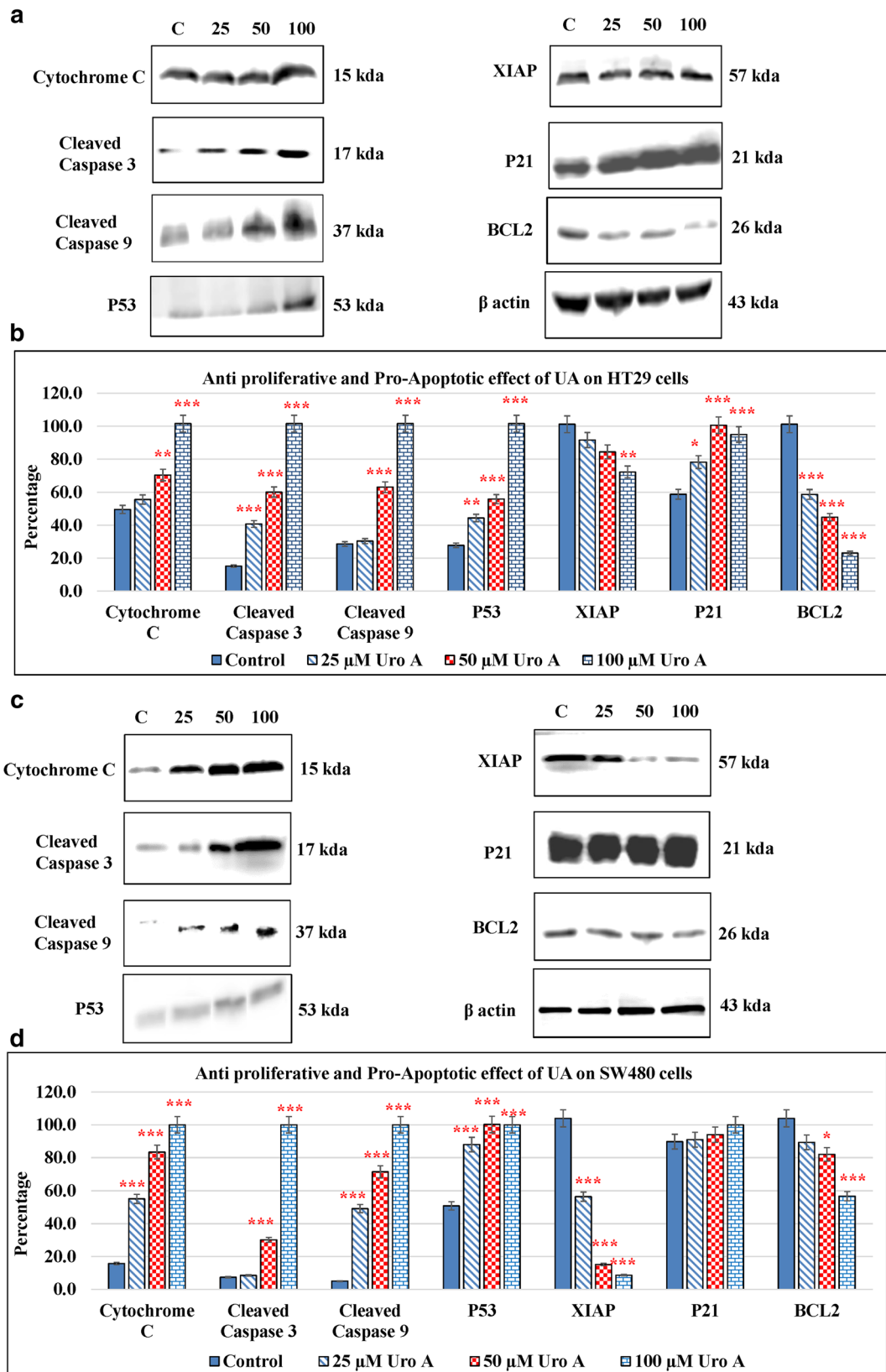


Fig. 5 Effect of UA on pro- and anti-apoptotic proteins. The three cancer cells were treated with 25 μ M, 50 μ M, and 100 μ M of UA, and cells were incubated for 48 h. Western blotting was performed, densitometry of the resulting bands was measured by ImageJ software, and the statistical

analysis was performed where the significance of data was assessed at P value < 0.05 . **a** and **b**, HT29. **c** and **d**, SW480. **e** and **f**, SW620. **g** and **h**, Normal fibroblasts

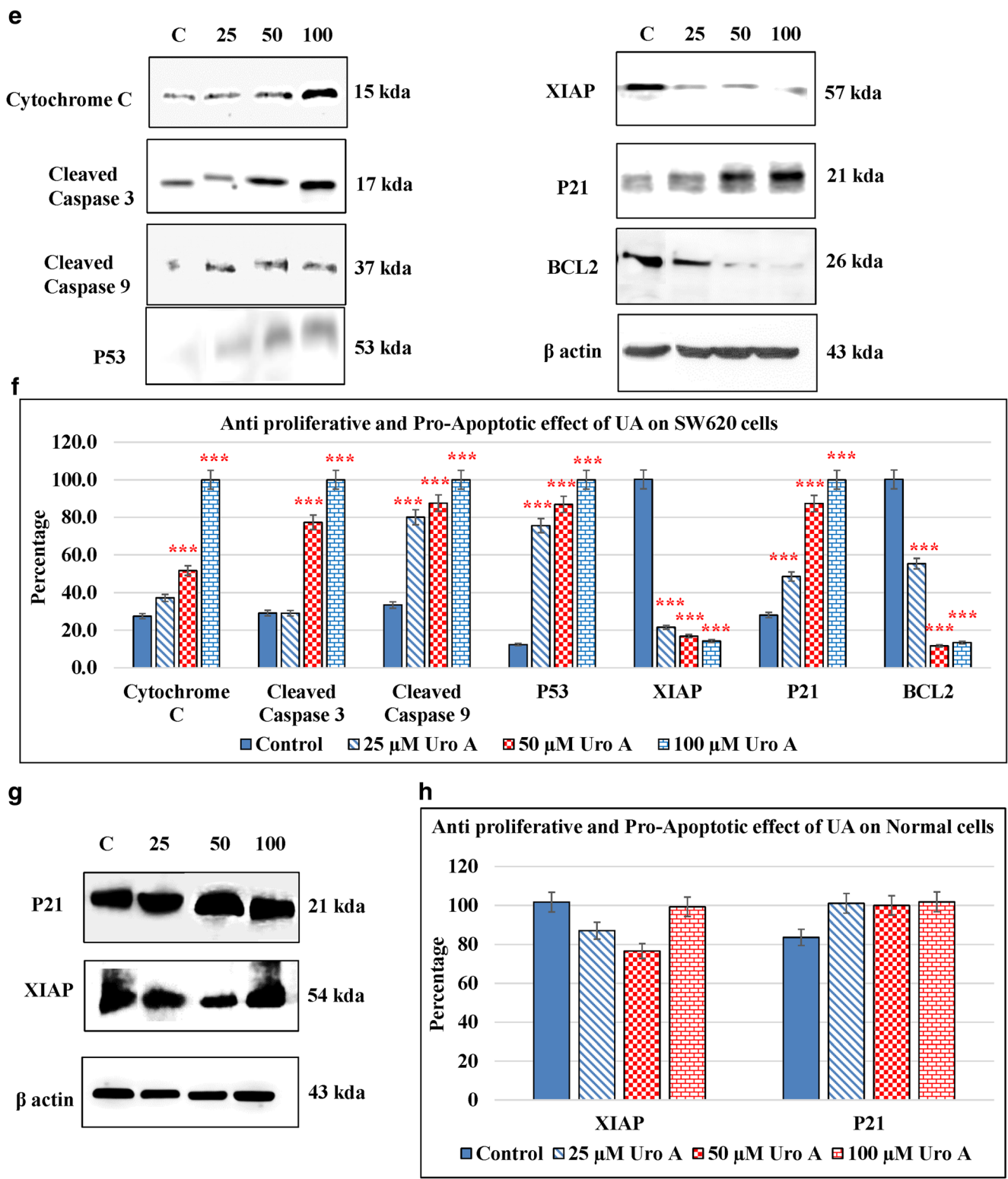


Fig. 5 continued

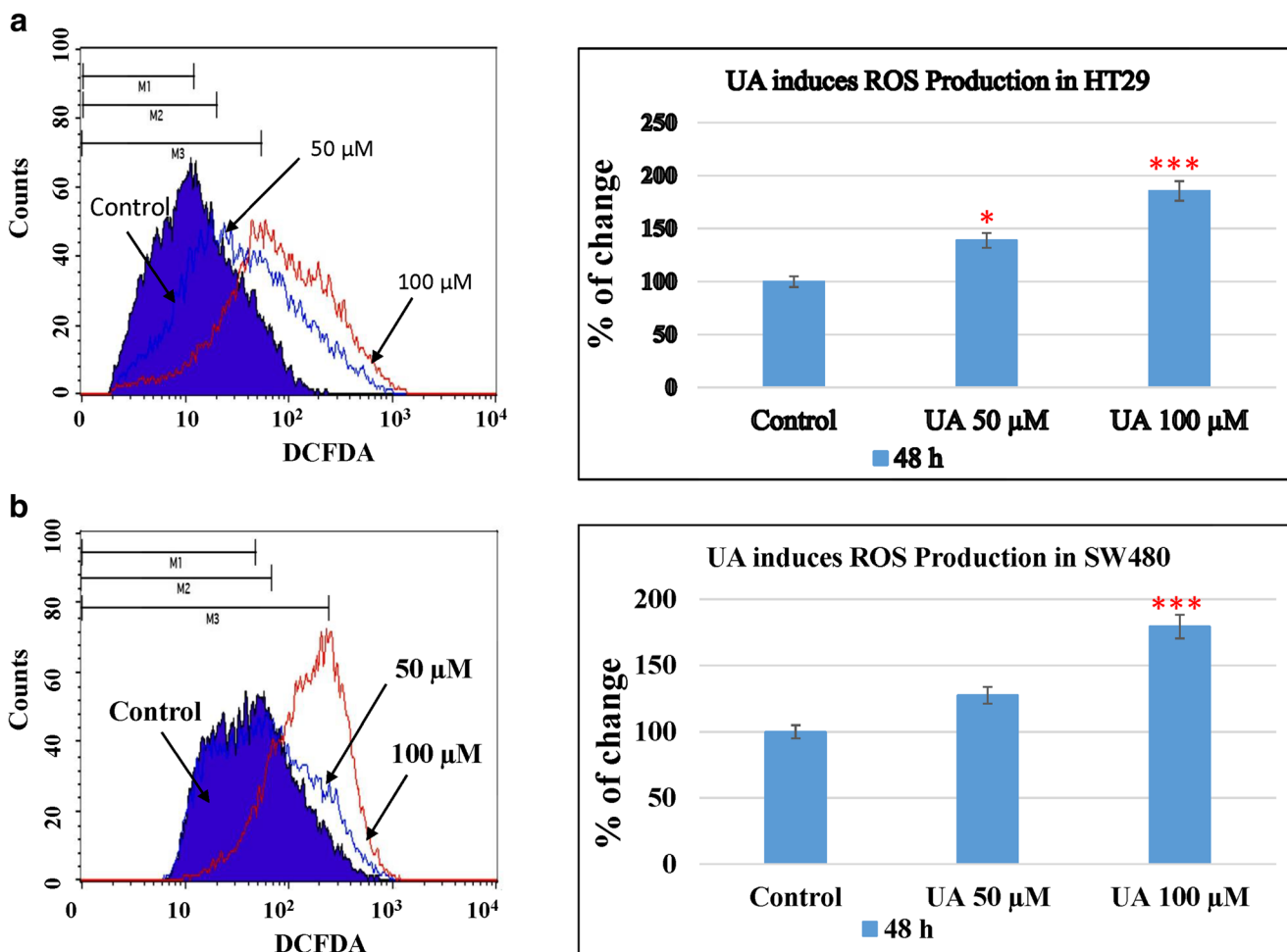


Fig. 6 UA induces ROS production in the colon cancer cells. Two concentrations of UA (50 μ M and 100 μ M) in addition to one untreated plate as a control were used to test its effect by oxidation of DCFDA in the three cancer cell lines in addition to the normal fibroblasts. The effect occurred at 24 h post-treatment. The effect was calculated

numerically by calculating the percentage of the markers (M1, M2, and M3) indicating the different peaks in the histograms of the control, 50 μ M, and 100 μ M, respectively. The statistical analysis was performed where the significance of data was assessed at a P value < 0.05. **a** HT29. **b** SW480. **c** SW620. **d** Normal fibroblasts

human bladder cancer T24 cells (Qiu et al. 2013), hepatocellular carcinomas HepG2 cells (Wang et al. 2015), human neuroblastoma SH-SY5Y cells (González-Sarrías et al. 2017b), and LNCaP prostate cancer cells (Sánchez-González et al. 2014, 2016).

Our results further showed that the cancer cells exposed to UA significantly upregulated the expression levels of cytochrome *c* with remarkable activation of caspase-3 and caspase-9, in a dose-dependent manner. These findings may indicate the release of cytochrome *c* in the cytoplasm after maximal levels had been reached in the mitochondria while the activation of caspase-3 and caspase-9 into the cytosol might activate the apoptotic pathway (Sharma et al. 2019). Caspase-9 functions as an apoptosis inhibitor by interfering with the N-terminal caspase recruitment domain (CARD) interaction between procaspase-9 and the apoptosis protease-activating factor-1 (Apaf-1), the main constituent of the apoptosome (Wang

et al. 2017). Previous studies showed that UA significantly increased caspase-3 levels by approximately 2-fold along with elevated peroxisome proliferator-activated receptor (PPAR- α) protein expression in human bladder cancer T24 cells (Qiu et al. 2013), hepatocellular carcinomas HepG2 cells (Wang et al. 2015), human neuroblastoma cells (González-Sarrías et al. 2017b), and prostate cancer cells (Sánchez-González et al. 2016). In colon cancer, a previous study on HT29 cells showed that UA induced the activation of caspase-3/9 cascade, cleavage of PARP, and induced mitochondrial membrane potential (Cho et al. 2015). Another study included the treatment of Caco-2, SW480, and HT29 cells with UA as a chemotherapy adjuvant of 5-fluorouracil and showed that UA induced a slight increase in caspase 8 and 9 activations (González-Sarrías et al. 2015).

The cell cycle has multiple, well-identified phases (G0/G1, S, and G2/M) through which the cells grow and replicate

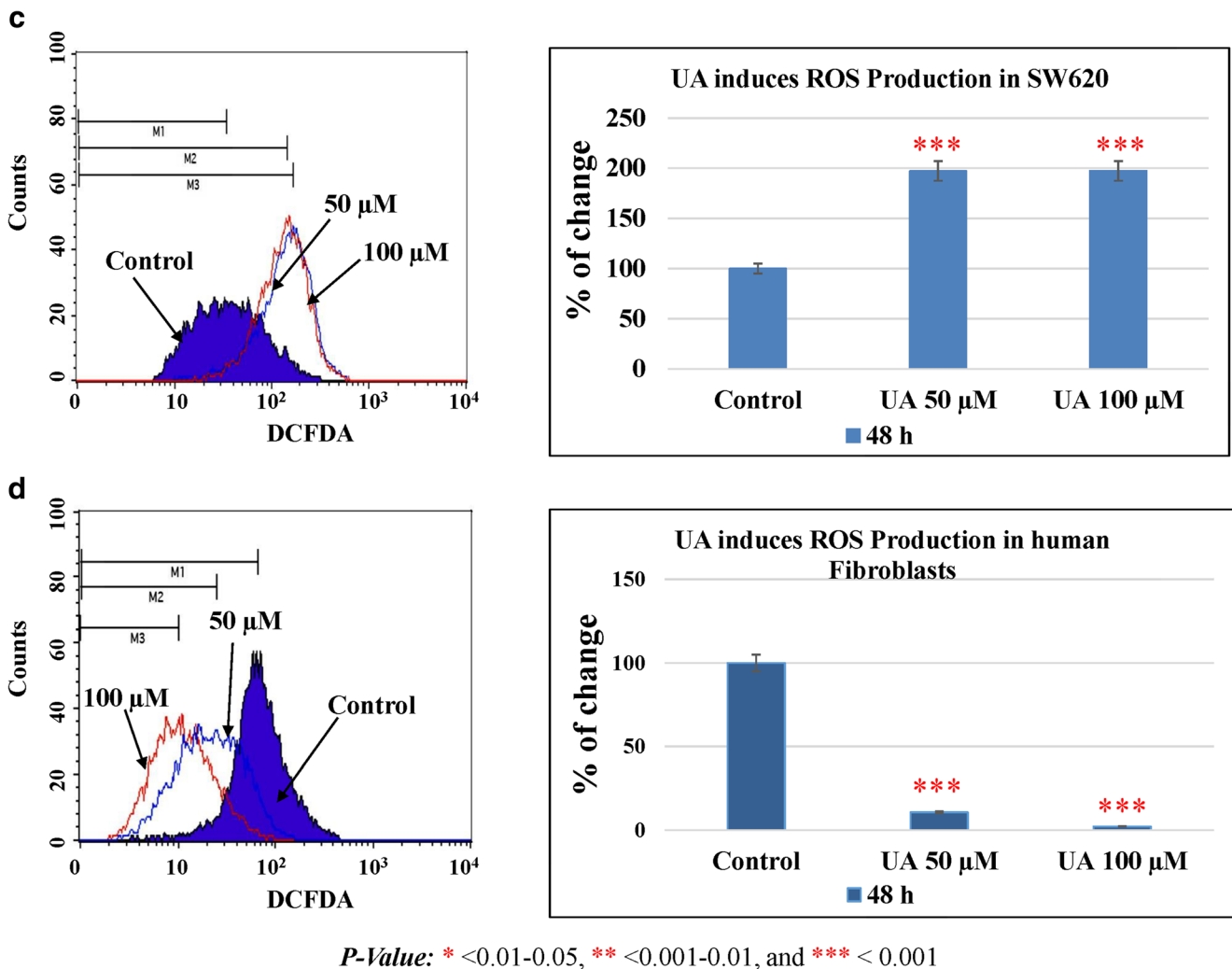


Fig. 6 continued

mainly regulated by cyclin proteins controlling the repeated cycles of cellular synthesis and degradation in the living organisms. These phases are regulated by cyclin-dependent kinases as well, which are activated by the upregulation of cyclin proteins. Cyclin D and CDK4/6 are the regulators of G0/G1 phase which initiate mitosis and cyclin E, and CDK2 regulates the S phase at which DNA is replicated, while cyclin A and cyclin B with CDK2 and CDK1, respectively, regulate the progression of mitosis and cytokinesis through S phase and drive entry from G2 into M phase (Kipreos and van den Heuvel 2019). The cell cycle arrest is the deactivation of one or more of the cell cycle phases induced by the use of chemicals or genetic manipulation which is regulated by the activation of p53 in tumor cells (Chen 2016). Our results showed that the CRC cells treated with UA were arrested at the G2/M phase with a clear reduction of G0/G1 phases. Furthermore, UA induced the upregulation of cyclin B1 with remarkable increases in the CDK6 levels as an indicator of cyclin D activation. Several studies showed that UA induces

cell cycle arrest at the G2/M phase in the UMUC3 bladder cancer cells (Liberal et al. 2017), prostate cancer cells with upregulation of cyclin B1 (Vicinanza et al. 2013), colon cancer cells Caco-2 (González-Sarriás et al. 2017b), HT29 (Cho et al. 2015), SW480 (González-Sarriás et al. 2016), SW620 (Zhao et al. 2018), and HCT116 cells (Norden and Heiss 2019). In contrast with our findings, a previous study reported that UA induced a cell cycle arrest at the G0/G1 phase in the prostate cancer cells LNCaP (Sánchez-González et al. 2016). Additionally, another study on the liver cancer cells HepG2 showed that UA decreased the levels of cyclin D (Wang et al. 2015). All of these reports may indicate the differential behavior of UA due to the type of cancer and cell context.

It is widely known that the apoptosis pathway is regulated by the extrinsic pathway and the intrinsic pathway depending on the involvement of mitochondria, controlled by the Bcl-2 and p53 gene families (Ghatei et al. 2017). Bcl-2 is an apoptotic regulator that inhibits the release of cytochrome c into the cytoplasm from mitochondria (Roufayel 2016). P53 has a

key role in the cell cycle arrest in the late G1 phase (Aubrey et al. 2018). XIAP (X-linked inhibitor of apoptosis) is an apoptosis inhibitor that binds to the initiator caspase-9, -3, and -7 resulting in their downregulation (Yang et al. 2018). P21 is the CDK inhibitor that promotes cell cycle arrest by both p53-dependent and p53-independent mechanisms, besides its primary role in transcriptional regulation, modulation, or inhibition of apoptosis depending on direct p21 protein interactions and its subcellular localizations (Karimian et al. 2016). P21 is mediated by Bcl-xL and p53 which regulate cell invasion and apoptosis (Kim et al. 2017). In the current study, our results showed the upregulation of p21 and p53 while the levels of Bcl-2 and XIAP decreased in all CRC cell lines. In agreement with our findings are the reports that UA induces p53 upregulation in the liver cancer cells HepG2 (Wang et al. 2015), and in the colon cancer cells HCT116 (Norden and Heiss 2019), and the upregulation of p21 in prostate cancer cells (Sánchez-González et al. 2016) and HT29 colon cancer cells (Cho et al. 2015). Another study showed that UA induced a 14% increase in the apoptotic cell population in LNCaP cells with a significant reduction in Bcl-2 protein levels (Sánchez-González et al. 2014). To the best of our knowledge, this is the first study to represent the effect of UA on the regulation of XIAP, p53, and Bcl-2 proteins in colon cancer cells.

To further confirm the molecular mechanism of the apoptotic and antiproliferative effect of UA, we sought to elucidate the effect of UA on oxidative stress in the colon cancer cells. ROS is the result of electron reductions of oxygen induced by cellular enzymes which leads to oxidative stress and DNA damage. Moreover, ROS can trigger or mediate the carcinogenesis of the initiation of tumorigenesis (Yokoyama et al. 2017). It was observed that most chemotherapeutics used in the treatment of different types of cancers induced elevated intracellular levels of ROS and redox-homeostasis alteration which progressed into cell death and apoptosis (Yang et al. 2018). In the present study, UA induced ROS production in the colon cancer cells. Ours is the first report showing that UA might affect cellular oxidation status as it can be considered an inducer of oxidative stress, inducing a toxic effect on the colon cancer cells leading to cellular apoptosis and cell death. At the same time and in contrast, UA did not affect the normal fibroblasts. In contrast to our findings, previous studies have shown that UA was considered an antioxidant by decreasing the ROS production in human bladder cancer T24 cells (Qiu et al. 2013) and the liver cancer cells HepG2 (Wang et al. 2015). Other studies supported our hypothesis that UA might cause elevation of ROS production as reported for the human neuroblastoma SH-SY5Y cell which showed increased REDOX activity; however, it decreased the oxidative stress-induced apoptosis by preventing caspase-3 activation (González-Sarrías et al. 2017b). There are no known studies that have investigated its effect on colon cancer cells.

Overall, our results suggest that UA had an inhibitory effect on cell proliferation and cell cycle distribution in the colon cancer cell line in a dose-dependent manner. UA induced a robust pro-apoptotic behavior which increased the total cell death rate through regulating the cellular caspases and apoptotic suppressors. UA induced cell arrest at the G2/M phase which indicated the DNA damage, confirmed by elevated levels of cyclin B1 and CDK6. Our novel findings show that UA increased the cellular oxidative stress accompanied by elevated levels of caspases-3 and -9 which led to cell death.

Supplementary Information The online version contains supplementary material available at <https://doi.org/10.1007/s12192-020-01189-8>.

Acknowledgments The authors are grateful to the Deanship of Scientific Research, King Saud University, for funding through the Vice Deanship of Scientific Research Chairs.

Author contributions RA, MSE, and MA contributed to the conception and conducting of the study and manuscript writing. IR, HH, and MIR performed the data analysis; MSE, M-A V-M, KAK, and TBT performed the experiments.

Compliance with ethical standards

Conflict of interest The authors declare that they have no conflict of interest.

Authors' approval All the authors agree and approve the manuscript.

References

- Afrin S, Giampieri F, Gasparrini M, Forbes-Hernández TY, Cianciosi D, Reboredo-Rodríguez P, Zhang J, Manna PP, Daglia M, Atanasov AG, Battino M (2020) Dietary phytochemicals in colorectal cancer prevention and treatment: a focus on the molecular mechanisms involved. *Biotechnol Adv* 38:107322. <https://doi.org/10.1016/j.biotechadv.2018.11.011>
- Ahmed K, Zaidi SF, Cui ZG, Zhou D, Saeed SA, Inadera H (2019) Potential proapoptotic phytochemical agents for the treatment and prevention of colorectal cancer. *Oncol Lett* 18(1):487–498. <https://doi.org/10.3892/ol.2019.10349>
- Alam MN, Almoyad M, Huq F (2018) Polyphenols in colorectal cancer: current state of knowledge including clinical trials and molecular mechanism of action. *Biomed Res Int* 2018:4154185–4154129. <https://doi.org/10.1155/2018/4154185>
- Al-Ishaq RK, Overy AJ, Büsselberg D (2020) Phytochemicals and gastrointestinal cancer: cellular mechanisms and effects to change cancer progression. *Biomolecules* 10(1):105. <https://doi.org/10.3390/biom10010105>
- André T, de Gramont A, Vernerey D, Chibaudel B, Bonnetain F, Tijeras-Raballand A, Scriver A, Hickish T, Tabernero J, van Laethem JL, Banzi M, Maartense E, Shmueli E, Carlsson GU, Scheithauer W, Papamichael D, Möehler M, Landolfi S, Demetter P, Colote S, Tournigand C, Louvet C, Duval A, Fléjou JF, de Gramont A (2015) Adjuvant fluorouracil, leucovorin, and oxaliplatin in stage

- II to III colon cancer: updated 10-year survival and outcomes according to BRAF mutation and mismatch repair status of the MOSAIC study. *J Clin Oncol* 33(35):4176–4187. <https://doi.org/10.1200/JCO.2015.63.4238>
- Aragonès G, Danesi F, Del Rio D, Mena P (2017) The importance of studying cell metabolism when testing the bioactivity of phenolic compounds. *Trends Food Sci Technol* 69(Part B):230–242. <https://doi.org/10.1016/j.tifs.2017.02.001>
- Aubrey BJ, Kelly GL, Janic A, Herold MJ, Strasser A (2018) How does p53 induce apoptosis and how does this relate to p53-mediated tumour suppression? *Cell Death Differ* 25(1):104–113. <https://doi.org/10.1038/cdd.2017.169>
- Bai J, Li Y, Zhang G (2017) Cell cycle regulation and anticancer drug discovery. *Cancer Biol Med* 14(4):348–362. <https://doi.org/10.20892/j.issn.2095-3941.2017.0033>
- Bray F, Ferlay J, Soerjomataram I, Siegel RL, Torre LA, Jemal A (2018) Global cancer statistics 2018: GLOBOCAN estimates of incidence and mortality worldwide for 36 cancers in 185 countries. *CA Cancer J Clin* 68(6):394–424. <https://doi.org/10.3322/caac.21492>
- Cai X, Zheng Y, Speck NA (2018) A Western blotting protocol for small numbers of hematopoietic stem cells. *J Vis Exp* 138:56855. <https://doi.org/10.3791/56855>
- Campbell KJ, Tait SWG (2018) Targeting BCL-2 regulated apoptosis in cancer. *Open Biol* 8(5):180002. <https://doi.org/10.1098/rsob.180002>
- Ceci C, Lacal PM, Tentori L, De Martino MG, Miano R, Graziani G (2018) Experimental evidence of the antitumor, antimetastatic and antiangiogenic activity of ellagic acid. *Nutrients* 10(11):1756. <https://doi.org/10.3390/nu10111756>
- Chen J (2016) The cell-cycle arrest and apoptotic functions of p53 in tumor initiation and progression. *Cold Spring Harb Perspect Med* 6(3):a026104. <https://doi.org/10.1101/cshperspect.a026104>
- Cho H, Jung H, Lee H, Yi HC, Kwak HK, Hwang KT (2015) Chemopreventive activity of ellagitannins and their derivatives from black raspberry seeds on HT29 colon cancer cells. *Food Funct* 6(5):1675–1683. <https://doi.org/10.1039/c5fo00274e>
- Conteduca V, Gurioli G, Rossi L, Scarpi E, Lolli C, Schepisi G, Farolfi A, de Lisi D, Gallà V, Burgio SL, Menna C, Amadori A, Losi L, Amadori D, Costi MP, de Giorgi U (2018) Oxaliplatin plus leucovorin and 5-fluorouracil (FOLFOX-4) as a salvage chemotherapy in heavily-pretreated platinum-resistant ovarian cancer. *BMC Cancer* 18(1):1267. <https://doi.org/10.1186/s12885-018-5180-1>
- Crowley LC, Waterhouse NJ (2016) Detecting cleaved caspase-3 in apoptotic cells by flow cytometry. *Cold Spring Harb Protoc* 2016(11):pdb.prot087312. <https://doi.org/10.1101/pdb.prot087312>
- Crowley LC, Marfell BJ, Scott AP, Waterhouse NJ (2016) Quantitation of apoptosis and necrosis by annexin V binding, propidium iodide uptake, and flow cytometry. *Cold Spring Harb Protoc* 2016(11):pdb.prot087288. <https://doi.org/10.1101/pdb.prot087288>
- Degirmencioglu S, Tanriverdi O, Demiray AG, Senol H, Dogu GG, Yaren A (2019) Retrospective comparison of efficacy and safety of CAPOX and FOLFOX regimens as adjuvant treatment in patients with stage III colon cancer. *J Int Med Res* 47(6):2507–2515. <https://doi.org/10.1177/0300060519848258>
- Degl'Innocenti D, Ramazzotti M, Sarchielli E, Monti D, Chevanne M, Vannelli GB, Barletta E (2019) Oxadiazon affects the expression and activity of aldehyde dehydrogenase and acylphosphatase in human striatal precursor cells: a possible role in neurotoxicity. *Toxicology* 411:110–121. <https://doi.org/10.1016/j.tox.2018.10.021>
- El-Deiry WS (2016) p21 (WAF1) mediates cell-cycle inhibition, relevant to cancer suppression and therapy. *Cancer Res* 76(18):5189–5191. <https://doi.org/10.1158/0008-5472.CAN-16-2055>
- Eskra JN, Schlicht MJ, Bosland MC (2019) Effects of black raspberries and their ellagic acid and anthocyanin constituents on taxane chemotherapy of castration-resistant prostate cancer cells. *Sci Rep* 9(1):4367. <https://doi.org/10.1038/s41598-019-39589-1>
- Espín JC, Larrosa M, García-Conesa MT, Tomás-Barberán F (2013) Biological significance of urolithins, the gut microbial ellagic acid-derived metabolites: the evidence so far. *Evid Based Complement Alternat Med* 2013:270418–270415. <https://doi.org/10.1155/2013/270418>
- Ghatei N, Sadr Nabavi A, Bahreyni Toosi M et al (2017) Evaluation of bax, Bcl-2, p21 and p53 genes expression variations on cerebellum of BALB/c mice before and after birth under mobile phone radiation exposure. *Iran J Basic Med Sci* 20(9):1037–1041. <https://doi.org/10.22038/IJBMS.2017.9273>
- González-Sarriás A, Larrosa M, Tomás-Barberán FA, Dolara P, Espín JC (2010) NF-kappaB-dependent anti-inflammatory activity of urolithins, gut microbiota ellagic acid-derived metabolites, in human colonic fibroblasts. *Br J Nutr* 104(4):503–512. <https://doi.org/10.1017/S0007114510000826>
- González-Sarriás A, Tomé-Carneiro J, Bellesia A, Tomás-Barberán FA, Espín JC (2015) The ellagic acid-derived gut microbiota metabolite, urolithin A, potentiates the anticancer effects of 5-fluorouracil chemotherapy on human colon cancer cells. *Food Funct* 6(5):1460–1469. <https://doi.org/10.1039/c5fo00120j>
- González-Sarriás A, Núñez-Sánchez MÁ, Tomé-Carneiro J, Tomás-Barberán FA, García-Conesa MT, Espín JC (2016) Comprehensive characterization of the effects of ellagic acid and urolithins on colorectal cancer and key-associated molecular hallmarks: MicroRNA cell specific induction of CDKN1A (p21) as a common mechanism involved. *Mol Nutr Food Res* 60(4):701–716. <https://doi.org/10.1002/mnfr.201500780>
- González-Sarriás A, Núñez-Sánchez MÁ, García-Villalba R, Tomás-Barberán FA, Espín JC (2017a) Antiproliferative activity of the ellagic acid-derived gut microbiota isourolithin A and comparison with its urolithin A isomer: the role of cell metabolism. *Eur J Nutr* 56(2):831–841. <https://doi.org/10.1007/s00394-015-1131-7>
- González-Sarriás A, Núñez-Sánchez MÁ, Tomás-Barberán FA, Espín JC (2017b) Neuroprotective effects of bioavailable polyphenol-derived metabolites against oxidative stress-induced cytotoxicity in human neuroblastoma SH-SY5Y cells. *J Agric Food Chem* 65(4):752–758. <https://doi.org/10.1021/acs.jafc.6b04538>
- Hammond WA, Swaika A, Mody K (2016) Pharmacologic resistance in colorectal cancer: a review. *Ther Adv Med Oncol* 8(1):57–84. <https://doi.org/10.1177/1758834015614530>
- Heilman J, Andreux P, Tran N, Rinsch C, Blanco-Bose W (2017) Safety assessment of urolithin A, a metabolite produced by the human gut microbiota upon dietary intake of plant derived ellagitannins and ellagic acid. *Food Chem Toxicol* 108(Pt A):289–297. <https://doi.org/10.1016/j.fct.2017.07.050>
- Ismail T, Calcabrini C, Diaz AR, Fimognari C, Turrini E, Catanzaro E, Akhtar S, Sestili P (2016) Ellagitannins in cancer chemoprevention and therapy. *Toxins (Basel)* 8(5):151. <https://doi.org/10.3390/toxins8050151>
- Karimian A, Ahmadi Y, Yousefi B (2016) Multiple functions of p21 in cell cycle, apoptosis and transcriptional regulation after DNA damage. *DNA Repair* 42:63–71. <https://doi.org/10.1016/j.dnarep.2016.04.008>
- Kasimsetty SG, Bialonska D, Reddy MK, Ma G, Khan S, Ferreira D (2010) Colon cancer chemopreventive activities of pomegranate ellagitannins and urolithins. *J Agric Food Chem* 58(4):2180–2187. <https://doi.org/10.1021/jf903762h>

- Kim KH, Sederstrom JM (2015) Assaying cell cycle status using flow cytometry. *Curr Protoc Mol Biol* 111:28.6.1–28.6.11. <https://doi.org/10.1002/0471142727.mb2806s111>
- Kim EM, Jung CH, Kim J, Hwang SG, Park JK, Um HD (2017) The p53/p21 complex regulates cancer cell invasion and apoptosis by targeting Bcl-2 family proteins. *Cancer Res* 77(11):3092–3100. <https://doi.org/10.1158/0008-5472.CAN-16-2098>
- Kipreos ET, van den Heuvel S (2019) Developmental control of the cell cycle: insights from *Caenorhabditis elegans*. *Genetics* 211(3):797–829. <https://doi.org/10.1534/genetics.118.301643>
- Kühlbrandt W (2015) Structure and function of mitochondrial membrane protein complexes. *BMC Biol* 13:89. <https://doi.org/10.1186/s12915-015-0201-x>
- Larrosa M, González-Sarriás A, Yáñez-Gascón MJ, Selma MV, Azorín-Ortuño M, Toti S, Tomás-Barberán F, Dolara P, Espín JC (2010) Anti-inflammatory properties of a pomegranate extract and its metabolite urolithin-A in a colitis rat model and the effect of colon inflammation on phenolic metabolism. *J Nutr Biochem* 21(8):717–725. <https://doi.org/10.1016/j.jnutbio.2009.04.012>
- Li P, Zhou L, Zhao T et al (2017) Caspase-9: structure, mechanisms and clinical application. *Oncotarget* 8(14):23996–24008. <https://doi.org/10.18632/oncotarget.15098>
- Liberal J, Carmo A, Gomes C, Cruz MT, Batista MT (2017) Urolithins impair cell proliferation, arrest the cell cycle and induce apoptosis in UMUC3 bladder cancer cells. *Investig New Drugs* 35(6):671–681. <https://doi.org/10.1007/s10637-017-0483-7>
- Liu Z, Jiang Z, Gao Y, Wang L, Chen C, Wang X (2019) TP53 mutations promote immunogenic activity in breast cancer. *J Oncol* 2019:5952836–5952819. <https://doi.org/10.1155/2019/5952836>
- Luparello C, Ragona D, Asaro DML, Lazzara V, Affranchi F, Celi M, Arizza V, Vazzana M (2019) Cytotoxic potential of the coelomic fluid extracted from the sea cucumber *Holothuria tubulosa* against triple-negative MDA-MB231 breast Cancer cells. *Biology (Basel)* 8(4):76. <https://doi.org/10.3390/biology8040076>
- Medic N, Tramer F, Passamonti S (2019) Anthocyanins in Colorectal Cancer Prevention. A systematic review of the literature in search of molecular oncotargets. *Front Pharmacol* 10:675. <https://doi.org/10.3389/fphar.2019.00675>
- Menyhárt O, Harami-Papp H, Sukumar S, Schäfer R, Magnani L, de Barrios O, Györfy B (2016) Guidelines for the selection of functional assays to evaluate the hallmarks of cancer. *Biochim Biophys Acta* 1866(2):300–319. <https://doi.org/10.1016/j.bbcan.2016.10.002>
- Moga MA, Dimienescu OG, Arvatescu CA, Mironescu A, Dracea L, Ples L (2016) The role of natural polyphenols in the prevention and treatment of cervical cancer-an overview. *Molecules* 21(8):1055. <https://doi.org/10.3390/molecules21081055>
- Napolitano S, Martini G, Rinaldi B, Martinelli E, Donniacuo M, Berrino L, Vitagliano D, Morgillo F, Barra G, de Palma R, Merolla F, Ciardiello F, Troiani T (2015) Primary and acquired resistance of colorectal cancer to anti-EGFR monoclonal antibody can be overcome by combined treatment of regorafenib with cetuximab. *Clin Cancer Res* 21(13):2975–2983. <https://doi.org/10.1158/1078-0432.CCR-15-0020>
- Norden E, Heiss EH (2019) Urolithin A gains in antiproliferative capacity by reducing the glycolytic potential via the p53/TIGAR axis in colon cancer cells. *Carcinogenesis* 40(1):93–101. <https://doi.org/10.1093/carcin/bgy158>
- Qiu Z, Zhou B, Jin L, Yu H, Liu L, Liu Y, Qin C, Xie S, Zhu F (2013) In vitro antioxidant and antiproliferative effects of ellagic acid and its colonic metabolite, urolithins, on human bladder cancer T24 cells. *Food Chem Toxicol* 59:428–437. <https://doi.org/10.1016/j.fct.2013.06.025>
- Rawla P, Sunkara T, Barsouk A (2019) Epidemiology of colorectal cancer: incidence, mortality, survival, and risk factors. *Prz Gastroenterol* 14(2):89–103. <https://doi.org/10.5114/pg.2018.81072>
- Roufayel R (2016) Regulation of stressed-induced cell death by the Bcl-2 family of apoptotic proteins. *Mol Membr Biol* 33(6–8):89–99. <https://doi.org/10.1080/09687688.2017.1400600>
- Sánchez-González C, Ciudad CJ, Noé V, Izquierdo-Pulido M (2014) Walnut polyphenol metabolites, urolithins A and B, inhibit the expression of the prostate-specific antigen and the androgen receptor in prostate cancer cells. *Food Funct* 5(11):2922–2930. <https://doi.org/10.1039/c4fo00542b>
- Sánchez-González C, Ciudad CJ, Izquierdo-Pulido M, Noé V (2016) Urolithin A causes p21 up-regulation in prostate cancer cells. *Eur J Nutr* 55(3):1099–1112. <https://doi.org/10.1007/s00394-015-0924-z>
- Sharma A, Boise LH, Shanmugam M (2019) Cancer metabolism and the evasion of apoptotic cell death. *Cancers (Basel)* 11(8):1144. <https://doi.org/10.3390/cancers11081144>
- Tchoghndjian A, Soubéran A, Tabouret E, Colin C, Denicolaï E, Jiguet-Jiglaire C, el-Battari A, Villard C, Baeza-Kallee N, Figarella-Branger D (2016) Inhibitor of apoptosis protein expression in glioblastomas and their in vitro and in vivo targeting by SMAC mimetic GDC-0152. *Cell Death Dis* 7(8):e2325. <https://doi.org/10.1038/cddis.2016.214>
- Van der Jeught K, Xu HC, Li YJ, Lu XB, Ji G (2018) Drug resistance and new therapies in colorectal cancer. *World J Gastroenterol* 24(34):3834–3848. <https://doi.org/10.3748/wjg.v24.i34.3834>
- Vicinanza R, Zhang Y, Henning SM, Heber D (2013) Pomegranate juice metabolites, ellagic acid and urolithin a, synergistically inhibit androgen-independent prostate cancer cell growth via distinct effects on cell cycle control and apoptosis. *Evid Based Complement Alternat Med* 2013:247504–247512. <https://doi.org/10.1155/2013/247504>
- Wang Y, Qiu Z, Zhou B, Liu C, Ruan J, Yan Q, Liao J, Zhu F (2015) In vitro antiproliferative and antioxidant effects of urolithin A, the colonic metabolite of ellagic acid, on hepatocellular carcinomas HepG2 cells. *Toxicol in Vitro* 29(5):1107–1115. <https://doi.org/10.1016/j.tiv.2015.04.008>
- Wang Y, Zhang Q, Zhong L, Lin M, Luo X, Liu S, Xu P, Liu X, Zhu YZ (2017) Apoptotic protease activating factor-1 inhibitor mitigates myocardial ischemia injury via disturbing procaspase-9 recruitment by Apaf-1. *Oxidative Med Cell Longev* 2017:9747296–9747299. <https://doi.org/10.1155/2017/9747296>
- Yang W, Zhou H, Yan Y (2018) XIAP underlies apoptosis resistance of renal cell carcinoma cells. *Mol Med Rep* 17:125–130. <https://doi.org/10.3892/mmr.2017.7925>
- Yin TF, Wang M, Qing Y, Lin YM, Wu D (2016) Research progress on chemopreventive effects of phytochemicals on colorectal cancer and their mechanisms. *World J Gastroenterol* 22(31):7058–7068. <https://doi.org/10.3748/wjg.v22.i31.7058>
- Yokoyama C, Sueyoshi Y, Ema M, Mori Y, Takaishi K, Hisatomi H (2017) Induction of oxidative stress by anticancer drugs in the presence and absence of cells. *Oncol Lett* 14(5):6066–6070. <https://doi.org/10.3892/ol.2017.6931>
- Yuzugulen J, Noshadi B, Shukur K, Sahin M, Gulcan H (2019) The metabolites of ellagitannin metabolism urolithins display various biological activities. *EMU J Pharm Sci* 2(2):102–110 Retrieved from: <https://dergipark.org.tr/en/pub/emujpharmsci/issue/51343/650678>
- Zhang S, Xue H, Chen Q (2016) Oxaliplatin, 5-fluorouracil and leucovorin (FOLFOX) as second-line therapy for patients with advanced urothelial cancer. *Oncotarget* 7:58579–58585. <https://doi.org/10.18632/oncotarget.10463>

- Zhang Y, Chen X, Gueydan C, Han J (2018) Plasma membrane changes during programmed cell deaths. *Cell Res* 28(1):9–21. <https://doi.org/10.1038/cr.2017.133>
- Zhang S, Al-Maghout T, Cao H et al (2019) Gut bacterial metabolite urolithin A (UA) mitigates Ca^{2+} entry in T cells by regulating miR-10a-5p. *Front Immunol* 10:1737. <https://doi.org/10.3389/fimmu.2019.01737>
- Zhao W, Shi F, Guo Z, Zhao J, Song X, Yang H (2018) Metabolite of ellagitannins, urolithin A induces autophagy and inhibits metastasis in human SW620 colorectal cancer cells. *Mol Carcinog* 57(2):193–200. <https://doi.org/10.1002/mc.22746>

Publisher's note Springer Nature remains neutral with regard to jurisdictional claims in published maps and institutional affiliations.